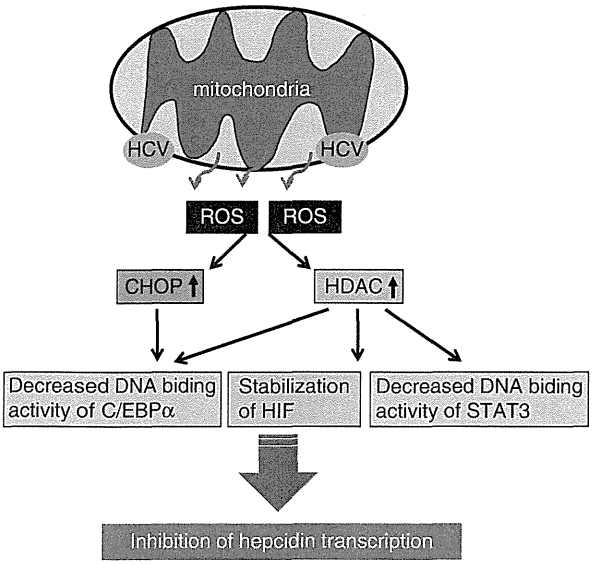

Figure 3 Schematic diagram depicting the mechanism by which mitochondrial reactive oxygen species (ROS) suppress hepcidin transcription in transgenic mice expressing hepatitis C virus (HCV) polyprotein or full-length HCV replicon cells. CHOP, CCAAT/enhancer-binding protein (C/EBP) homology protein; HDAC, histone deacetylase; HIF, hypoxia inducible factor; STAT3, signal transduction and activator of transcription 3.

transgenic mice expressing the HCV polyprotein.[75] There are several lines of evidence indicating that ROS upregulate the expression of CHOP.[76] In agreement with our observation, an *in vitro* study using hepatoma cells showed that HCV-induced ROS inhibited the binding activity of C/EBPα and signal transduction and activator of transcription 3 to the hepcidin promoter in addition to stabilization of hypoxia-inducible factor through increased histone deacetylase activity.[77] Thus, HCV core-induced mitochondrial ROS accumulate hepatic iron through the inhibition of hepcidin transcription (Fig. 3).

CONCLUSION

IN THE PRESENT review we discussed how HCV interacts with mitochondria and how subsequently occurring mitochondrial ROS production contributes to the pathophysiology of HCV-related chronic liver diseases. The mitochondrion is the key organelle that determines the cellular response to various kinds of biological stress. Therefore, it may not be surprising that HCV-induced alterations of mitochondrial functions have a critical impact on disease progression towards hepatocarcinogenesis by creating an oxidatively stressed liver microenvironment through mitochondrial ROS production. However, the molecular details underlying HCV-induced mitochondrial dysfunctions remain confusing and are still a matter of debate, which undoubtedly requires further investigation to shed light on the questions in this field.

ACKNOWLEDGMENTS

THIS RESEARCH WAS supported by a Grant-in-Aid for Scientific Research (B) (no. 23390201) from the Japan Society for the Promotion of Science, by a Health and Labor Sciences Research Grant for Research on Hepatitis from the Ministry of Health, Labor and Welfare of Japan and by a P2 Research Project Grant from Kawasaki Medical School.

REFERENCES

1 Poynard T, Yuen MF, Ratziu V, Lai CL. Viral hepatitis C. *Lancet* 2003; **362:** 2095–100.
2 Seeff LB. Natural history of chronic hepatitis C. *Hepatology* 2002; **36:** S35–46.
3 Farinati F, Cardin R, De Maria N *et al.* Iron storage, lipid peroxidation and glutathione turnover in chronic anti-HCV positive hepatitis. *J Hepatol* 1995; **22:** 449–56.
4 Barbaro G, Di Lorenzo G, Asti AM *et al.* Hepatocellular mitochondrial alterations in patients with chronic hepatitis C: ultrastructural and biochemical findings. *Am J Gastroenterol* 1999; **942:** 198–205.
5 Valgimigli M, Valgimigli L, Trere D *et al.* Oxidative stress EPR measurement in human liver by radical-probe technique. Correlation with etiology, histology and cell proliferation. *Free Radic Res* 2002; **36:** 939–48.
6 Kitase A, Hino K, Furutani T *et al.* In situ detection of oxidized n-3 polyunsaturated fatty acids in chronic hepatitis C: correlation with hepatic steatosis. *J Gastroenterol* 2005; **40:** 617–24.
7 Moriya K, Nakagawa K, Santa T *et al.* Oxidative stress in the absence of inflammation in a mouse model for hepatitis C virus-associated hepatocarcinogenesis. *Cancer Res* 2001; **61:** 4365–70.
8 Okuda M, Li K, Beard MR *et al.* Mitochondrial injury, oxidative stress, and antioxidant gene expression are induced by hepatitis C virus core protein. *Gastroenterology* 2002; **122:** 366–75.
9 Otani K, Korenaga M, Beard MR *et al.* Hepatitis C virus core protein, cytochrome P450 2E1, and alcohol produce combined mitochondrial injury and cytotoxicity in hepatoma cells. *Gastroenterology* 2005; **128:** 96–107.

10 Korenaga M, Wang T, Li Y *et al.* Hepatitis C virus core protein inhibits mitochondrial electron transport and increases reactive oxygen species (ROS) production. *J Biol Chem* 2005; **280**: 37481–8.
11 Ando M, Korenaga M, Hino K *et al.* Mitochondrial electron transport inhibition in full genomic hepatitis C virus replicon cells is restored by reducing viral replication. *Liver Int* 2008; **28**: 1158–66.
12 Allison ME, Wreghitt T, Palmer CR, Alexander GJ. Evidence for a link between hepatitis C virus infection and diabetes mellitus in a cirrhotic population. *J Hepatol* 1994; **21**: 1135–9.
13 Caronia S, Taylor K, Pagliaro L *et al.* Further evidence for an association between non-insulin-dependent diabetes mellitus and chronic hepatitis C virus infection. *Hepatology* 1999; **30**: 1059–63.
14 Mason AL, Lau JY, Hoang N *et al.* Association of diabetes mellitus and chronic hepatitis C virus infection. *Hepatology* 1999; **29**: 328–33.
15 Moriya K, Yotsuyanagi H, Shintani Y *et al.* Hepatitis C virus core protein induces hepatic steatosis in transgenic mice. *J Gen Virol* 1997; **78**: 1527–31.
16 Rubbia-Brandt L, Quadri R, Abid K *et al.* Hepatocyte steatosis is a cytopathic effect of hepatitis C virus genotype 3. *J Hepatol* 2000; **33**: 106–15.
17 Kageyama F, Kobayashi Y, Kawasaki T, Toyokuni S, Uchida K, Nakamura H. Successful interferon therapy reverses enhanced hepatic iron accumulation and lipid peroxidation in chronic hepatitis C. *Am J Gastroenterol* 2000; **95**: 1041–50.
18 Davila JA, Morgan RO, Shaib Y, McGlynn KA, El-Serag HB. Diabetes increases the risk of hepatocellular carcinoma in the United States: a population based case control study. *Gut* 2005; **54**: 533–9.
19 Moriya K, Fujie H, Shintani Y *et al.* The core protein of hepatitis C virus induces hepatocellular carcinoma in transgenic mice. *Nat Med* 1998; **4**: 1065–7.
20 Lerat H, Honda M, Beard MR *et al.* Steatosis and liver cancer in transgenic mice expressing the structural and nonstructural proteins of hepatitis C virus. *Gastroenterology* 2002; **122**: 352–65.
21 Kato J, Miyanishi K, Kobune M *et al.* Long-term phlebotomy with low-iron diet therapy lowers risk of development of hepatocellular carcinoma from chronic hepatitis C. *J Gastroenterol* 2007; **42**: 830–6.
22 Fisher-Wellman KH, Neufer PD. Linking mitochondrial bioenergetics to insulin resistance via redox biology. *Trends Endocrinol Metab* 2012; **23**: 142–53.
23 Schwer B, Ren S, Pietschmann T *et al.* Targeting of hepatitis C virus core protein to mitochondria through a novel C-terminal localization motif. *J Virol* 2004; **78**: 7958–68.
24 Chu VC, Bhattacharya S, Nomoto A *et al.* Persistent expression of hepatitis C virus non-structural proteins leads to increased autophagy and mitochondrial injury in human hepatoma cells. *PLoS ONE* 2011; **6**: e28551.
25 Wang T, Campbell RV, Yi MK, Lemon SM, Weinman SA. Role of Hepatitis C virus core protein in viral-induced mitochondrial dysfunction. *J Viral Hepat* 2010; **17**: 784–93.
26 Rouille Y, Helle F, Delgrange D *et al.* Subcellular localization of hepatitis C virus structural proteins in a cell culture system that efficiently replicates the virus. *J Virol* 2006; **80**: 2832–41.
27 Brault C, Levy PL, Bartosch B. Hepatitis C virus-induced mitochondrial dysfunctions. *Viruses* 2013; **5**: 954–80.
28 Tsutsumi T, Matsuda M, Aizaki H *et al.* Proteomics analysis of mitochondrial proteins reveals overexpression of a mitochondrial protein chaperon, prohibitin, in cells expressing hepatitis C virus core protein. *Hepatology* 2009; **50**: 378–86.
29 Abdalla MY, Ahmad IM, Spitz DR, Schmidt WN, Britigan BE. Hepatitis C virus-core and nonstructural proteins lead to different effects on cellular antioxidant defenses. *J Med Virol* 2005; **76**: 489–97.
30 Morbitzer M, Herget T. Expression of gastrointestinal glutathione peroxidase is inversely correlated to the presence of hepatitis C virus subgenomic RNA in human liver cells. *J Biol Chem* 2005; **280**: 8831–41.
31 Machida K, Cheng KT, Lai CK, Jeng KS, Sung VM, Lai MM. Hepatitis C virus triggers mitochondrial permeability transition with production of reactive oxygen species, leading to DNA damage and STAT3 activation. *J Virol* 2006; **80**: 7199–207.
32 Li K, Prow T, Lemon SM, Beard MR. Cellular response to conditional expression of hepatitis C virus core protein in Huh7 cultured human hepatoma cells. *Hepatology* 2002; **35**: 1237–46.
33 Boudreau HE, Emerson SU, Korzeniowska A, Jendrysik MA, Leto TL. Hepatitis C virus (HCV) proteins induce NADPH oxidase 4 expression in a transforming growth factor beta-dependent manner: a new contributor to HCV-induced oxidative stress. *J Virol* 2009; **83**: 12934–46.
34 deMochel NS, Seronello S, Wang SH *et al.* Hepatocyte NAD(P)H oxidases as an endogenous source of reactive oxygen species during hepatitis C virus infection. *Hepatology* 2010; **52**: 47–59.
35 Rieusset J, Fauconnier J, Paillard M *et al.* Disruption of cyclophilin d-mediated calcium transfer from the ER to mitochondria contributes to hepatic ER stress and insulin resistance. *Hepatology* 2013; **58**: 1195.
36 Balaban RS. Cardiac energy metabolism homeostasis: role of cytosolic calcium. *J Mol Cell Cardiol* 2002; **34**: 1259–71.
37 Gong G, Waris G, Tanveer R, Siddiqui A. Human hepatitis C virus NS5A protein alters intracellular calcium levels, induces oxidative stress, and activates STAT-3 and NF-kappa B. *Proc Natl Acad Sci U S A* 2001; **98**: 9599–604.
38 Li Y, Boehning DF, Qian T, Popov VL, Weinman SA. Hepatitis C virus core protein increases mitochondrial ROS production by stimulation of Ca2+ uniporter activity. *FASEB J* 2007; **21**: 2474–85.

39 Piccoli C, Scrima R, Quarato G *et al.* Hepatitis C virus protein expression causes calcium-mediated mitochondrial bioenergetic dysfunction and nitro-oxidative stress. *Hepatology* 2007; **46**: 58–65.
40 Maher P. Redox control of neural function: background, mechanisms, and significance. *Antioxid Redox Signal* 2006; **8**: 1941–70.
41 Narendra D, Tanaka A, Suen DF *et al.* Parkin is recruited selectively to impaired mitochondria and promotes their autophagy. *J Cell Biol* 2008; **183**: 795–803.
42 Youle RJ, Narendra DP. Mechanisms of mitophagy. *Nat Rev Mol Cell Biol* 2011; **12**: 9–14.
43 Kurihara Y, Kanki T, Aoki Y *et al.* Mitophagy plays an essential role in reducing mitochondrial production of reactive oxygen species and mutation of mitochondrial DNA by maintaining mitochondrial quantity and quality in yeast. *J Biol Chem* 2012; **287**: 3265–72.
44 Elmore SP, Qian T, Grissom S *et al.* The mitochondrial permeability transition initiates autophagy in rat hepatocytes. *FASEB J* 2001; **15**: 2286–7.
45 Geisler S, Holmstrom KM, Skujat D *et al.* PINK1/Parkin-mediated mitophagy is dependent on VDAC1 and p62/SQSTM1. *Nat Cell Biol* 2010; **12**: 119–31.
46 Kim SJ, Syed GH, Siddiqui A. Hepatitis C virus induces the mitochondrial translocation of Parkin and subsequent mitophagy. *PLoS Pathog* 2013; **9**: e1003285.
47 Hui JM, Sud A, Farrell GC *et al.* Insulin resistance is associated with chronic hepatitis C virus infection and fibrosis progression. *Gastroenterology* 2003; **125**: 1695–704.
48 Aytug S, Reich D, Sapiro LE, Bernstein D, Begum N. Impaired IRS-1/PI3-kinase signaling in patients with HCV: a mechanism for increased prevalence of type 2 diabetes. *Hepatology* 2003; **38**: 1384–92.
49 Shintani Y, Fujie H, Miyoshi H *et al.* Hepatitis C virus infection and diabetes: direct involvement of the virus in the development of insulin resistance. *Gastroenterology* 2004; **126**: 840–8.
50 Kawaguchi T, Yoshida T, Harada M *et al.* Hepatitis C virus down-regulates insulin receptor substrates 1 and 2 through up-regulation of suppressor of cytokine signaling 3. *Am J Pathol* 2004; **165**: 1499–508.
51 Shlomai A, Rechtman MM, Burdelova EO *et al.* The metabolic regulator PGC-1alpha links hepatitis C virus infection to hepatic insulin resistance. *J Hepatol* 2012; **57**: 867–73.
52 Emanuelli B, Peraldi P, Filloux C, Sawka-Verhelle D, Hilton D, Van Obberghen E. SOCS-3 is an insulin-induced negative regulator of insulin signaling. *J Biol Chem* 2000; **275**: 15985–91.
53 Ueki K, Kondo T, Kahn CR. Suppressor of cytokine signaling 1 (SOCS-1) and SOCS-3 cause insulin resistance through inhibition of tyrosine phosphorylation of insulin receptor substrate proteins by discrete mechanisms. *Mol Cell Biol* 2004; **24**: 5434–46.
54 Hotamisligil GS, Peraldi P, Budavari A, Ellis R, White MF, Spiegelman BM. IRS-1-mediated inhibition of insulin receptor tyrosine kinase activity in TNF-alpha- and obesity-induced insulin resistance. *Science* 1996; **271**: 665–8.
55 Aguirre V, Werner ED, Giraud J, Lee YH, Shoelson SE, White MF. Phosphorylation of Ser307 in insulin receptor substrate-1 blocks interactions with the insulin receptor and inhibits insulin action. *J Biol Chem* 2002; **277**: 1531–7.
56 Copps KD, Hancer NJ, Opare-Ado L, Qiu W, Walsh C, White MF. Irs1 serine 307 promotes insulin sensitivity in mice. *Cell Metab* 2010; **11**: 84–92.
57 Chiarugi P. PTPs versus PTKs: the redox side of the coin. *Free Radic Res* 2005; **39**: 353–64.
58 Tonks NK. Redox redux: revisiting PTPs and the control of cell signaling. *Cell* 2005; **121**: 667–70.
59 Boura-Halfon S, Zick Y. Phosphorylation of IRS proteins, insulin action, and insulin resistance. *Am J Physiol Endocrinol Metab* 2009; **296**: E581–91.
60 Houstis N, Rosen ED, Lander ES. Reactive oxygen species have a causal role in multiple forms of insulin resistance. *Nature* 2006; **440**: 944–8.
61 Michael MD, Kulkarni RN, Postic C *et al.* Loss of insulin signaling in hepatocytes leads to severe insulin resistance and progressive hepatic dysfunction. *Mol Cell* 2000; **6**: 87–97.
62 Moriya K, Todoroki T, Tsutsumi T *et al.* Increase in the concentration of carbon 18 monounsaturated fatty acids in the liver with hepatitis C: analysis in transgenic mice and humans. *Biochem Biophys Res Commun* 2001; **281**: 1207–12.
63 Perlemuter G, Sabile A, Letteron P *et al.* Hepatitis C virus core protein inhibits microsomal triglyceride transfer protein activity and very low density lipoprotein secretion: a model of viral-related steatosis. *FASEB J* 2002; **16**: 185–94.
64 Moriishi K, Mochizuki R, Moriya K *et al.* Critical role of PA28gamma in hepatitis C virus-associated steatogenesis and hepatocarcinogenesis. *Proc Natl Acad Sci U S A* 2007; **104**: 1661–6.
65 Furutani T, Hino K, Okuda M *et al.* Hepatic iron overload induces hepatocellular carcinoma in transgenic mice expressing the hepatitis C virus polyprotein. *Gastroenterology* 2006; **130**: 2087–98.
66 Fenton HJH. Oxidation of tartaric acid in presence of iron. *J Chem Soc* 1894; **65**: 899–910.
67 Shibutani S, Takeshita M, Grollman AP. Insertion of specific bases during DNA synthesis past the oxidation-damaged base 8-oxodG. *Nature* 1991; **349**: 431–4.
68 Fujita N, Horiike S, Sugimoto R *et al.* Hepatic oxidative DNA damage correlates with iron overload in chronic hepatitis C patients. *Free Radic Biol Med* 2007; **42**: 353–62.
69 Hentze MW, Muckenthaler MU, Andrews NC. Balancing acts: molecular control of mammalian iron metabolism. *Cell* 2004; **117**: 285–97.
70 Krause A, Neitz S, Magert HJ *et al.* LEAP-1, a novel highly disulfide-bonded human peptide, exhibits antimicrobial activity. *FEBS Lett* 2000; **480**: 147–50.

71 Park CH, Valore EV, Waring AJ, Ganz T. Hepcidin, a urinary antimicrobial peptide synthesized in the liver. *J Biol Chem* 2001; **276**: 7806–10.
72 Fujita N, Sugimoto R, Takeo M *et al.* Hepcidin expression in the liver: relatively low level in patients with chronic hepatitis C. *Mol Med* 2007; **13**: 97–104.
73 Girelli D, Pasino M, Goodnough JB *et al.* Reduced serum hepcidin levels in patients with chronic hepatitis C. *J Hepatol* 2009; **51**: 845–52.
74 Harrison-Findik DD, Schafer D, Klein E *et al.* Alcohol metabolism-mediated oxidative stress down-regulates hepcidin transcription and leads to increased duodenal iron transporter expression. *J Biol Chem* 2006; **281**: 22974–82.
75 Nishina S, Hino K, Korenaga M *et al.* Hepatitis C virus-induced reactive oxygen species raise hepatic iron level in mice by reducing hepcidin transcription. *Gastroenterology* 2008; **134**: 226–38.
76 Bek MF, Bayer M, Muller B *et al.* Expression and function of C/EBP homology protein (GADD153) in podocytes. *Am J Pathol* 2006; **168**: 20–32.
77 Miura K, Taura K, Kodama Y, Schnabl B, Brenner DA. Hepatitis C virus-induced oxidative stress suppresses hepcidin expression through increased histone deacetylase activity. *Hepatology* 2008; **48**: 1420–9.

OPEN ACCESS Freely available online

PLOS | ONE

New Susceptibility and Resistance HLA-DP Alleles to HBV-Related Diseases Identified by a Trans-Ethnic Association Study in Asia

Nao Nishida[1,2*9], Hiromi Sawai[2,9], Koichi Kashiwase[3], Mutsuhiko Minami[3], Masaya Sugiyama[1], Wai-Kay Seto[4], Man-Fung Yuen[4], Nawarat Posuwan[5], Yong Poovorawan[5], Sang Hoon Ahn[6], Kwang-Hyub Han[6], Kentaro Matsuura[7], Yasuhito Tanaka[7], Masayuki Kurosaki[8], Yasuhiro Asahina[9,10], Namiki Izumi[8], Jong-Hon Kang[11], Shuhei Hige[12], Tatsuya Ide[13], Kazuhide Yamamoto[14], Isao Sakaida[15], Yoshikazu Murawaki[16], Yoshito Itoh[17], Akihiro Tamori[18], Etsuro Orito[19], Yoichi Hiasa[20], Masao Honda[21], Shuichi Kaneko[21], Eiji Mita[22], Kazuyuki Suzuki[23], Keisuke Hino[24], Eiji Tanaka[25], Satoshi Mochida[26], Masaaki Watanabe[27], Yuichiro Eguchi[28], Naohiko Masaki[1], Kazumoto Murata[1], Masaaki Korenaga[1], Yoriko Mawatari[1], Jun Ohashi[29], Minae Kawashima[2], Katsushi Tokunaga[2], Masashi Mizokami[1]*

1 The Research Center for Hepatitis and Immunology, National Center for Global Health and Medicine, Ichikawa, Chiba, Japan, **2** Department of Human Genetics, Graduate School of Medicine, The University of Tokyo, Bunkyo-ku, Tokyo, Japan, **3** HLA Laboratory, Japanese Red Cross Kanto-Koshinetsu Block Blood Center, Koutou-ku, Tokyo, Japan, **4** Department of Medicine, Queen Mary Hospital, Hong Kong, **5** Faculty of Medicine, Chulalongkorn University, Bangkok, Thailand, **6** Department of Internal Medicine, Yonsei University College of Medicine, Seoul, South Korea, **7** Department of Virology & Liver Unit, Nagoya City University Graduate School of Medical Sciences, Nagoya, Aichi, Japan, **8** Division of Gastroenterology and Hepatology, Musashino Red Cross Hospital, Musashino, Tokyo, Japan, **9** Department of Liver Disease Control, Tokyo Medical and Dental University, Bunkyo-ku, Tokyo, Japan, **10** Department of Gastroenterology and Hepatology, Tokyo Medical and Dental University, Bunkyo-ku, Tokyo, Japan, **11** Department of Internal Medicine, Teine Keijinkai Hospital, Sapporo, Hokkaido, Japan, **12** Department of Internal Medicine, Hokkaido University Graduate School of Medicine, Sapporo, Hokkaido, Japan, **13** Division of Gastroenterology, Department of Medicine, Kurume University School of Medicine, Kurume, Fukuoka, Japan, **14** Department of Gastroenterology and Hepatology, Okayama University Graduate School of Medicine, Dentistry, and Pharmaceutical Sciences, Okayama, Okayama, Japan, **15** Gastroenterology and Hepatology, Yamaguchi University Graduate School of Medicine, Ube, Yamaguchi, Japan, **16** Faculty of Medicine, Tottori University, Tottori, Tottori, Japan, **17** Molecular Gastroenterology and Hepatology, Kyoto Prefectural University of Medicine, Kyoto, Kyoto, Japan, **18** Department of Hepatology, Osaka City University Graduate School of Medicine, Osaka, Osaka, Japan, **19** Department of Gastroenterology, Nagoya Daini Red Cross Hospital, Nagoya, Aichi, Japan, **20** Department of Gastroenterology and Metabology, Ehime University Graduate School of Medicine, Toon, Ehime, Japan, **21** Department of Gastroenterology, Kanazawa University Graduate School of Medicine, Kanazawa, Ishikawa, Japan, **22** Department of Gastroenterology and Hepatology, National Hospital Organization Osaka National Hospital, Osaka, Osaka, Japan, **23** Division of Gastroenterology and Hepatology, Department of Internal Medcine, Iwate Medical University, Morioka, Iwate, Japan, **24** Division of Hepatology and Pancreatology, Kawasaki Medical College, Kurashiki, Okayama, Japan, **25** Department of Medicine, Shinshu University School of Medicine, Matsumoto, Nagano, Japan, **26** Division of Gastroenterology and Hepatology, Saitama Medical University, Iruma, Saitama, Japan, **27** Department of Gastroenterology, Kitasato University School of Medicine, Sagamihara, Kanagawa, Japan, **28** Department of Internal Medicine, Saga Medical School, Saga, Saga, Japan, **29** Faculty of Medicine, University of Tsukuba, Tsukuba, Ibaraki, Japan

Abstract

Previous studies have revealed the association between SNPs located on human leukocyte antigen (*HLA*) class II genes, including *HLA-DP* and *HLA-DQ*, and chronic hepatitis B virus (HBV) infection, mainly in Asian populations. *HLA-DP* alleles or haplotypes associated with chronic HBV infection or disease progression have not been fully identified in Asian populations. We performed trans-ethnic association analyses of *HLA-DPA1*, *HLA-DPB1* alleles and haplotypes with hepatitis B virus infection and disease progression among Asian populations comprising Japanese, Korean, Hong Kong, and Thai subjects. To assess the association between *HLA-DP* and chronic HBV infection and disease progression, we conducted high-resolution (4-digit) *HLA-DPA1* and *HLA-DPB1* genotyping in a total of 3,167 samples, including HBV patients, HBV-resolved individuals and healthy controls. Trans-ethnic association analyses among Asian populations identified a new risk allele *HLA-DPB1*09:01* ($P = 1.36 \times 10^{-6}$; OR = 1.97; 95% CI, 1.50–2.59) and a new protective allele *DPB1*02:01* ($P = 5.22 \times 10^{-6}$; OR = 0.68; 95% CI, 0.58–0.81) to chronic HBV infection, in addition to the previously reported alleles. Moreover, *DPB1*02:01* was also associated with a decreased risk of disease progression in chronic HBV patients among Asian populations ($P = 1.55 \times 10^{-7}$; OR = 0.50; 95% CI, 0.39–0.65). Trans-ethnic association analyses identified Asian-specific associations of *HLA-DP* alleles and haplotypes with HBV infection or disease progression. The present findings will serve as a base for future functional studies of HLA-DP molecules in order to understand the pathogenesis of HBV infection and the development of hepatocellular carcinoma.

Citation: Nishida N, Sawai H, Kashiwase K, Minami M, Sugiyama M, et al. (2014) New Susceptibility and Resistance HLA-DP Alleles to HBV-Related Diseases Identified by a Trans-Ethnic Association Study in Asia. PLoS ONE 9(2): e86449. doi:10.1371/journal.pone.0086449

Editor: Ferruccio Bonino, University of Pisa, Italy

Received November 13, 2013; **Accepted** December 10, 2013; **Published** February 10, 2014

Funding: This work was supported by a Grant-in-Aid from the Ministry of Health, Labour, and Welfare of Japan H24-Bsou-kanen-ippan-011 and H24-kanen-ippan-004 to Masashi Mizokami, H23-kanen-005 to Katsushi Tokunaga, H25-kanen-wakate-013 to Nao Nishida, and H25-kanen-wakate-012 to Hiromi Sawai. This work was also supported by The Grant for National Center for Global Health and Medicine 22-shi-302 to Masashi Mizokami and 24-shi-107 to Nao Nishida. Partial support by Grant-in-Aid from the Ministry of Education, Culture, Sports, Science of Japan [grant number 22133008] for Scientific Research on Innovative Areas to Katsushi Tokunaga, [grant number 24790728] for Young Scientists (B) to Nao Nishida, and [grant number 25870178] for Young Scientists (B) to Hiromi Sawai, is also acknowledged. The funders had no role in study design, data collection and analysis, decision to publish, or preparation of the manuscript.

Competing Interests: The authors have declared that no competing interests exist.

* E-mail: mmizokami@hospk.ncgm.go.jp (MM); nishida-75@umin.ac.jp (NN)

☯ These authors contributed equally to this work.

Introduction

Hepatitis B virus (HBV) infection is a major global health problem, resulting in 0.5–1.0 million deaths per year [1]. The prevalence of chronic HBV infection varies. About 75% of the chronic carriers in the world live in Southeast Asia and East Pacific [2]. Due to the introduction of vaccination programs, the prevalence of HBV infection in many countries has gradually been decreasing with consequent decreases in HBV-related hepatocellular carcinoma (HCC) [3]. Although some HBV carriers spontaneously eliminate the virus, about 10–15% of carriers develop liver cirrhosis (LC), liver failure and HCC [4]. Moreover, the progression of liver disease was revealed to be associated with the presence of several distinct mutations in HBV infections [5]. Genetic variations in *STAT4* and *HLA-DQ* genes were recently identified as host genetic factors in a large-scale genome-wide association study (GWAS) for HBV-related HCC in China [6].

With regard to the genes associated with susceptibility to chronic HBV infection, *HLA-DP* and *HLA-DQ* genes were identified by GWAS in Japanese and Thai populations in 2009 [7] and 2011 [8], respectively. In addition, our previous GWAS confirmed and identified the association of SNP markers located on *HLA-DPA1* (rs3077) and *HLA-DPB1* (rs9277535) genes with susceptibility to chronic hepatitis B (CHB) and HBV clearance in Japanese and Korean subjects[9]. The significant associations of *HLA-DP* with CHB and HBV clearance have mainly been detected in Asian populations, such as Japanese [8,9], Thai [7], Chinese [10–12], and Korean [9]. In 2012, the association between *HLA-DPA1* gene SNPs and persistent HBV infection was replicated in a Germany non-Asian population for the first time; however, this showed no association with HBV infection [13]. These results seem to be explained by the fact that allele frequencies of both rs3077 (0.155, 0.587 and 0.743 for C allele, on HapMap CEU, JPT, and YRI) and rs9277535 (0.261, 0.558 and 0.103 for G allele, on HapMap CEU, JPT, and YRI) are markedly different between populations. Moreover, the previous study showed that HBsAg seropositivity rates were higher in Thailand and China (5–12%) than in North America and Europe (0.2–0.5%) [2]. These results suggest that comparative analyses of *HLA-DP* alleles and haplotypes in Asian populations would clarify key host factors of the susceptible and protective *HLA-DP* alleles and haplotypes for CHB and HBV clearance. Here, we performed trans-ethnic analyses of *HLA-DP* alleles and haplotypes in Asian populations comprising Japanese, Korean, Hong Kong and Thai individuals. The findings from this study will serve as a base for future functional studies of HLA-DP molecules.

Results

Characteristics of studied subjects

The characteristics of a total of 3,167 samples, including Japanese, Korean, Hong Kong and Thai subjects, are shown in Table 1. Each population included three groups of HBV patients, resolved individuals and healthy controls. The clinical definitions of HBV patients and resolved individuals are summarized in Materials and Methods. Some of the Japanese and all of the Korean samples overlapped with the subjects in our previous study [9,14].

We performed genotyping for *HLA-DPA1* and *HLA-DPB1* in all 3,167 samples, and a total of 2,895 samples were successfully genotyped. The characteristics of successfully genotyped samples are shown in Table S1.

Association of *HLA-DPA1* and *HLA-DPB1* alleles in Asian populations

As for a general Asian population, including 464 Japanese, 140 Korean, 156 Hong Kong, and 122 Thai subjects, five *HLA-DPA1* alleles and twenty-four *HLA-DPB1* alleles were observed (Table S2). The frequencies of *HLA-DPA1* and *HLA-DPB1* alleles were similar between Japanese and Korean subjects. On the other hand, the number of alleles with frequencies of 1–2% was larger in Hong Kong and Thai populations, despite the small sample size. Although the frequencies of *HLA-DP* alleles varied in Asian populations, *HLA-DPB1*05:01* was the most prevalent with over 30% in all populations.

The associations of *HLA-DPA1* and *HLA-DPB1* alleles with chronic HBV infection (i.e., comparison between HBV patients and healthy controls) are shown in Table S2. To avoid false positives caused by multiple testing, the significance levels were corrected based on the numbers of *HLA-DPA1* and *HLA-DPB1*

Table 1. Number of individuals in this study.

Population	Japanese	Korean	Hong Kong	Thai
Total number of samples	1,291	586	661	629
HBV patients	489	340	281	390
IC	114	-	-	-
CH	147	175	187	198
AE	21	-	-	-
LC	38	-	-	-
HCC	169	165	94	192
Mean age (y)	57.1	44.7	57.9	52.0
(min-max)	(20–84)	(18–74)	(32–86)	(21–84)
Gender (M/F)	338/151	265/75	239/42	289/101
Resolved individuals*	335	106	190	113
HCV (−)	249	106	190	113
HCV (+)	86	-	-	-
Mean age (y)	59.7	43.1	40.0	48.2
(min-max)	(18–87)	(12–66)	(18–60)	(39–66)
Gender (M/F)	173/162	61/45	113/77	83/30
Healthy controls	467	140	190	126
Mean age (y)	39.0**	33.7	26.2	46.6
(min-max)	(23–64)	(1–59)	(16–60)	(38–79)
Gender (M/F)	370/97	67/73	87/103	73/53

Abbreviation: IC, Inactive Carrier; CH, Chronic Hepatitis; AE, Acute Exacerbation; LC, Liver Cirrhosis; HCC, Hepatocellular Carcinoma.

* Resolved individuals were HBsAg negative and HBcAb positive.

** 419 of 467 healthy controls were de-identified, without information on age.

doi:10.1371/journal.pone.0086449.t001

alleles in the focal population. Briefly, the significance level was set at 0.05/(# of observed alleles at each locus) in each population (see Materials and Methods). With regard to high-risk alleles of *HLA-DPA1*, the most prevalent allele *HLA-DPA1*02:02* was significantly associated with susceptibility to HBV infection in Japanese ($P = 3.45 \times 10^{-4}$; OR = 1.39; 95% CI, 1.16–1.68) and Korean subjects ($P = 2.66 \times 10^{-5}$; OR = 1.89; 95% CI, 1.39–2.58), whereas this association was not observed in Hong Kong or Thai subjects. The association of *HLA-DPA1*02:01* with susceptibility to HBV infection was significant only in Japanese ($P = 2.61 \times 10^{-7}$; OR = 1.88; 95% CI, 1.46–2.41). The significant association of *HLA-DPA1*01:03* with protection against HBV infection was commonly observed among four Asian populations (Table S2). The pooled OR and 95% CI were 0.51 and 0.41–0.63, respectively in a meta-analysis ($P = 3.15 \times 10^{-10}$) (Fig. S1A).

As shown in Table S2, *HLA-DPB1* shows higher degree of polymorphism than *HLA-DPA1*. The most common allele in Asian populations, *HLA-DPB1*05:01*, was significantly associated with HBV susceptibility in both Japanese and Korean subjects. Although *HLA-DPB1*05:01* showed no significant association in the Hong Kong and Thai populations, the same direction of association (i.e., HBV susceptibility) was observed. Meta-analysis of the four populations revealed a significant association between *HLA-DPB1*05:01* and susceptibility to HBV infection ($P = 1.51 \times 10^{-4}$; OR = 1.45; 95% CI, 1.19–1.75) (Fig. S1B). The frequency of *HLA-DPB1*09:01* was significantly elevated in Japanese HBV patients (15.7%) as compared with healthy controls (8.7%) ($P = 3.70 \times 10^{-6}$; OR = 1.94; 95% CI, 1.45–2.62), and this association was most significant (i.e., the smallest P value) in the Japanese population. Because of lower allele frequencies of *HLA-DPB1*09:01* or lack of statistical power in the other populations, no significant associations were observed. A common allele in Thai subjects, *HLA-DPB1*13:01*, was significantly associated with susceptibility to HBV infection ($P = 2.49 \times 10^{-4}$; OR = 2.17; 95% CI, 1.40–3.47) with the same direction of associations in Japanese and Hong Kong (OR = 1.52 and 1.40, respectively).

*HLA-DPB1*04:02* was identified as the most protective allele for HBV infection in Japanese ($P = 1.59 \times 10^{-7}$; OR = 0.37; 95% CI, 0.24–0.55) and Korean subjects ($P = 1.27 \times 10^{-7}$; OR = 0.19; 95% CI, 0.10–0.38). Both *HLA-DPB1*02:01* and *HLA-DPB1*04:01* were also significantly associated with protection in the Japanese population, and the former was significantly associated with protection in Hong Kong subjects ($P = 9.17 \times 10^{-4}$; OR = 0.49; 95% CI, 0.32–0.76). This common allele among four Asian populations, *HLA-DPB1*02:01*, showed a significant association with protection against HBV infection ($P = 5.22 \times 10^{-6}$; OR = 0.68; 95% CI, 0.58–0.81) in a meta-analysis (Fig. S1B).

The frequencies of associated *HLA-DP* alleles in a comparison of HBV patients with healthy controls (Table S2) or with HBV-resolved individuals (Table S3) were similar in all four Asian populations. In the Japanese population, the associations of susceptible and protective *HLA-DPB1* alleles to chronic HBV infection seem weaker in the comparison of HBV patients with HBV-resolved individuals than in the comparison of HBV patients with healthy controls. Moreover, the results of association analyses showed no difference in the comparison of HBV patients with HBV-resolved individuals, including or excluding HCV positive individuals (Table S3). In contrast, the association became stronger in the comparison of HBV patients with HBV-resolved individuals among the Korean subjects. The protective allele *HLA-DPB1*04:01* was also identified to have a strong association with HBV clearance in Hong Kong subjects (Table S3). Moreover, in Hong Kong subjects, the *HLA-DPB1*05:01* associated with the risk for HBV infection showed lower frequency in HBV-resolved individuals (42.9%) than in the healthy controls (48.1%), which accounts for a strong association in the comparison of HBV patients with HBV-resolved individuals ($P = 6.24 \times 10^{-3}$; OR = 1.64; 95% CI, 1.14–2.36). Although the number of samples was insufficient, *HLA-DP*100:01* showed a significant association with protection against HBV infection in the Hong Kong population ($P = 3.05 \times 10^{-6}$; OR = 0.03; 95% CI, 0.0007–0.20).

Table 2. Association of number of *DPB1*02:01* alleles (i.e., 0, 1 or 2) with disease progression in CHB patients assessed by multivariate logistic regression analysis adjusted for age and sex.

Population	P value	OR (95% CI)
Japanese	0.000177	0.47 (0.32–0.70)
Korean	0.025358	0.55 (0.33–0.93)
Hong Kong	0.040842	0.46 (0.22–0.97)
Thai	0.087782	0.58 (0.31–1.08)
All*	1.55×10^{-7}	0.50 (0.39–0.65)

*Population was adjusted using dummy variables.

doi:10.1371/journal.pone.0086449.t002

As for disease progression in CHB patients among Asian populations, a protective effect of *HLA-DPB1*02:01* on disease progression was observed in the Japanese ($P = 4.26 \times 10^{-5}$; OR = 0.45; 95% CI, 0.30–0.67) and Korean populations ($P = 8.74 \times 10^{-4}$; OR = 0.47; 95% CI, 0.29–0.75) (Table S4). Multivariate logistic regression analysis adjusted for age and sex revealed that the number of *DPB1*02:01* alleles (i.e., 0, 1, or 2) was significantly associated with disease progression in CHB patients in Japanese ($P = 1.77 \times 10^{-4}$; OR = 0.47; 95% CI, 0.32–0.70) (Table 2). Moreover, protective effects of *DPB1*02:01* on disease progression in Asian populations ($P = 1.55 \times 10^{-7}$; OR = 0.50; 95% CI, 0.39–0.65) were detected in a multivariate logistic regression analysis adjusted for age, gender, and population (Table 2).

Associations of *DPA1-DPB1* haplotypes in Asian populations

The estimated frequencies of *HLA DPA1-DPB1* haplotypes are shown in Table S5. The most frequent haplotype among the four Asian populations was *DPA1*02:02-DPB1*05:01*. The number of haplotypes with low frequencies of 1–2% was 10 in both Japanese and Korean subjects, whereas more haplotypes appeared with frequencies of 1–2% in Hong Kong and Thai subjects. The associations of *DPA1-DPB1* haplotypes with HBV infection are shown in Table S5. In the Japanese population, *DPA1*02:01-DPB1*09:01* showed the most significant association with susceptibility to HBV infection ($P = 3.38 \times 10^{-6}$; OR = 1.95; 95% CI, 1.46–2.64). The most common haplotype in the four Asian populations, *DPA1*02:02-DPB1*05:01*, was found to be significantly associated with susceptibility to HBV infection in the Japanese and Korean subjects ($P = 7.40 \times 10^{-4}$; OR = 1.37; 95% CI, 1.14–1.66 for Japanese, and $P = 4.50 \times 10^{-6}$; OR = 2.02; 95% CI, 1.48–2.78 for Korean). In the Thai subjects, *HLA-DPB1*13:01* was the most significant risk allele for HBV infection (Table S2); however, no significant associations were found for the three different haplotypes bearing *HLA-DPB1*13:01*: *DPA1*02:01-DPB1*13:01*, *DPA1*02:02-DPB1*13:01*, and *DPA1*04:01-DPB1*13:01*,indicating that the association of *HLA-DPB1*13:01* with susceptibility to HBV infection did not result from a specific *DPA1-DPB1* haplotype or combination with a specific *DPA1* allele.

In the Japanese population, both haplotypes *DPA1*01:03-DPB1*04:01* and *DPA1*01:03-DPB1*04:02* showed significant associations with protection against HBV infection ($P = 1.17 \times 10^{-5}$; OR = 0.32; 95% CI, 0.18–0.56 for *DPA1*01:03-DPB1*04:01* and $P = 1.95 \times 10^{-7}$; OR = 0.37; 95% CI, 0.24–0.55 for *DPA1*01:03-DPB1*04:02*). In the Korean subjects, a significant association of *DPA1*01:03-DPB1*04:02* was also demonstrated; however, no association was observed for *DPA1*01:03-DPB1*04:01*. Because the observed number of each haplotype was small, none of the other haplotypes showed a significant association with protection against HBV infection.

In order to identify trans-ethnic DPA1-DPB1 haplotypes associated with HBV infection, a meta-analysis was performed. A meta-analysis further revealed that the *DPA1*01:03-DPB1*02:01* haplotype was significantly associated with protection against HBV infection ($P = 1.45 \times 10^{-5}$; OR = 0.69; 95% CI, 0.58–0.82) (Fig. S1C).

Discussion

Among 2.2 billion individuals worldwide who are infected with HBV, 15% of these are chronic carriers. Of chronic carriers, 10–15% develops LC, liver failure and HCC, and the remaining individuals eventually achieve a state of nonreplicative infection, resulting in HBsAg negative and anti-HBc positive, i.e. HBV-resolved individuals. To identify host genetic factors associated with HBV-related disease progression may lead HBV patients to discriminate individuals who need treatment.

The *HLA-DPA1* and *HLA-DPB1* genes were identified as host genetic factors significantly associated with CHB infection, mainly in Asian populations [7–12], and not in European populations [13]. In the previous association analyses of *HLA-DPB1* alleles with HBV infection, one risk allele *HLA-DPB1*05:01* (OR = 1.52; 95% CI, 1.31–1.76), and two protective alleles, *HLA-DPB1*04:01* (OR = 0.53; 95% CI, 0.34–0.80) and *HLA-DPB1*04:02* (OR = 0.47; 95% CI, 0.34–.64), were identified in the Japanese population [7]. In this study, we further identified a new risk allele *HLA-DPB1*09:01* (OR = 1.94; 95% CI, 1.45–2.62) for HBV infection and a new protective allele *HLA-DPB1*02:01* (OR = 0.71; 95% CI, 0.56–0.89) in the Japanese population, in addition to the previously reported alleles (Table S2) [7]. The discrepancy in the association of *HLA-DPB1*09:01* allele with risk for HBV infection in a previous study [7] results from the elevated frequency of *HLA-DPB1*09:01* in the controls (12.2%), which is higher than our controls (8.7%). In this study, healthy subjects were recruited as controls. In contrast, individuals that were registered in BioBank Japan as subjects with diseases other than CHB were recruited as controls in the previous study [7], which may have included patients with diseases with which *HLA-DPB1*09:01* is associated. Although no significant association of *HLA-DPB1*09:01* with risk for HBV infection was observed in the Korean subjects, *HLA-DPB1*09:01* appears to have a susceptible effect on HBV infection, as it showed the same direction of association. When the association analyses in Japanese and Korean subjects were combined in meta-analysis, the association was statistically significant ($P = 1.36 \times 10^{-6}$; OR = 1.97; 95% CI, 1.50–2.59). Thus, *HLA-DPB1*09:01* may be a Northeast Asian-specific allele associated with risk for HBV infection.

Moreover, a significant association of *HLA-DPB1*13:01* with risk of HBV infection (OR = 2.17; 95% CI, 1.40–3.47) was identified in the Thai subjects. However, the frequency of *HLA-DPB1*13:01* in Thai healthy controls (11.5% in the present study) reportedly varies, ranging from 15.4% to 29.5%, due to the population diversity [15–17]. Therefore, a replication analysis is required to confirm the association of *HLA-DPB1*13:01* with HBV infection in the Thai subjects. There were four other marginally associated *HLA-DPB1* alleles with low allele frequencies below 5% in HBV patients and healthy controls, including *HLA-DPB1*28:01*, *-DPB1*31:01*, *-DPB1*100:01*, and *-DPB1*105:01*, in the Hong Kong and Thai subjects. Because these infrequent alleles may have resulted from false positive associations, the association needs to be validated in a large number of subjects.

*HLA-DPB1*02:01* showed a significant association with protection against HBV infection in both Japanese and Hong Kong populations (Table S2); however, the *HLA-DPB1*02:01* allele was not associated with HBV infection in the previous study [7]. Although *HLA-DPB1*02:01* showed no association in either Korean or Thai populations, a significant association of *HLA-DPB1*02:01* with protection against HBV infection among four Asian populations was detected in meta-analysis ($P = 5.22 \times 10^{-6}$; OR = 0.68; 95% CI, 0.58–0.81) (Fig. S1B). We therefore conclude that the present finding is not a false positive.

A recent report showed that *HLA-DPB1*02:01:02*, **02:02*, **03:01:01*, **04:01:01*, **05:01*, **09:01*, and **14:01* were significantly associated with response to booster HB vaccination in Taiwan neonatally vaccinated adolescents [18]. The *HLA-DPB1*02:01:02*, **02:02*, **03:01:01*, **04:01:01*, and **14:01* were significantly more frequent in recipients whose post-booster titers of antibodies against HBV surface antigen (anti-HBs) were detectable, on the other hand, *HLA-DPB1*05:01* and **09:01* were significantly more frequent in recipients who were undetectable. Moreover, the *HLA-DPB1*05:01* and **09:01* significantly increase the likelihoods of undetectable pre-booster anti-HBs titers. These results seem consistent with our findings, in which *HLA-DPB1*05:01* and **09:01* are associated with susceptibility to chronic hepatitis B infection.

We also identified a protective effect of *HLA-DPB1*02:01* allele on disease progression in Asian populations. Previous studies identified the association of HLA class II genes including *HLA-DQ* and *HLA-DR* with development of HBV related hepatocellular carcinoma in the Chinese population [6,19,20]. In this study using Japanese and Korean samples, we identified significant associations between *HLA-DPB1*02:01* and disease progression in CHB patients ($P = 4.26 \times 10^{-5}$; OR = 0.45; 95% CI, 0.30–0.67, for Japanese and $P = 8.74 \times 10^{-4}$; OR = 0.47; 95% CI, 0.29–0.75 for Korean) (Table S4). Although the association of *HLA-DPB1*02:01* with disease progression was weaker after adjustment for age and gender in Korean subjects ($P = 2.54 \times 10^{-2}$; OR = 0.55; 95% CI, 0.33–0.93), the same direction of association was observed (i.e. protective effect on disease progression) (Table 2). The protective effects of *HLA-DPB1*02:01* on disease progression showed a significant association after adjustment for age and gender in the Japanese population ($P = 1.77 \times 10^{-4}$; OR = 0.47; 95% CI, 0.32–0.70); moreover, a significant association between *HLA-DPB1*02:01* was observed among four Asian populations, under which population was adjusted by using dummy variables in a multivariate logistic regression analysis ($P = 1.55 \times 10^{-7}$; OR = 0.50; 95% CI, 0.39–0.65) (Table 2).

The *HLA-DPA1* and *HLA-DPB1* belong to the HLA class II alpha and beta chain paralogues, which make a heterodimer consisting of an alpha and a beta chain on the surface of antigen presenting cells. This HLA class II molecule plays a central role in the immune system by presenting peptides derived from extracellular proteins. We identified two susceptible haplotypes (*DPA1*02:02-DPB1*05:01* and *DPA1*02:01-DPB1*09:01*) and three protective haplotypes (*DPA1*01:03-DPB1*04:01*, *DPA1*01:03-DPB1*04:02*, and *HLA-DPA1*01:03-DPB1*02:01*) to chronic hepatitis B infection, which may result in different binding

affinities between HLA-DP subtypes and extracellular antigens. Although functional analyses of HLA-DP subtypes to identify HBV-related peptides are not fully completed, identification of susceptible and protective haplotypes as host genetic factors would lead us to understand the pathogenesis of HBV infection including viral factors.

In summary, we identified a new risk allele *HLA-DPB1*09:01*, which was specifically observed in Northeast Asian populations, Japanese and Korean. Moreover, a new protective allele *HLA-DPB1*02:01* was identified among four Asian populations: Japanese, Korean, Hong Kong and Thai. The protective allele *HLA-DPB1*02:01* was associated with both chronic HBV infection and disease progression in chronic HBV patients. Identification of a total of five alleles, including two risk alleles (*DPB1*09:01* and *DPB1*05:01*) and three protective alleles (*DPB1*04:01*, *DPB1*04:02* and *DPB1*02:01*), would enable HBV-infected individuals to be classified into groups according to the treatment requirements. Moreover, the risk and protective alleles for HBV infection and disease progression, identified in this study by means of trans-ethnic association analyses, would be key host factors to recognize HBV-derived antigen peptides. The present results may lead to subsequent functional studies into HLA-DP molecules and viral factors in order to understand the pathogenesis of HBV infection and development of hepatocellular carcinoma.

Materials and Methods

Ethics Statement

All study protocols conform to the relevant ethical guidelines, as reflected in the *a priori* approval by the ethics committee of National Center for Global Health and Medicine, and by the ethics committees of all participating universities and hospitals, including The University of Tokyo, Japanese Red Cross Kanto-Koshinetsu Block Blood Center, The University of Hong Kong, Chulalongkorn University, Yonsei University College of Medicine, Nagoya City University Graduate School of Medical Sciences, Musashino Red Cross Hospital, Tokyo Medical and Dental University, Teine Keijinkai Hospital, Hokkaido University Graduate School of Medicine, Kurume University School of Medicine, Okayama University Graduate School of Medicine, Yamaguchi University Graduate School of Medicine, Tottori University, Kyoto Prefectural University of Medicine, Osaka City University Graduate School of Medicine, Nagoya Daini Red Cross Hospital, Ehime University Graduate School of Medicine, Kanazawa University Graduate School of Medicine, National Hospital Organization Osaka National Hospital, Iwate Medical University, Kawasaki Medical College, Shinshu University School of Medicine, Saitama Medical University, Kitasato University School of Medicine, Saga Medical School, and University of Tsukuba.

Written informed consent was obtained from each patient who participated in this study and all samples were anonymized. For Japanese healthy controls, 419 individuals were de-identified with information about gender, and all were recruited after obtaining verbal informed consent in Tokyo prior to 1990. For the 419 Japanese healthy individuals, written informed consent was not obtained because the blood sampling was conducted before the "Ethical Guidelines for Human Genome and Genetic Sequencing Research" were established in Japan. Under the condition that DNA sample is permanently de-linked from the individual, this study was approved by the Research Ethics Committee of National Center for Global Health and Medicine.

Characteristics of studied subjects

All of the 3,167 genomic DNA samples were collected from individuals with HBV, HBV-resolved individuals (HBsAg-negative and anti-HBc-positive) and healthy controls at 26 multi-center hospitals throughout Japan, Korea, Hong Kong, and Thailand (Table 1). In a total of 1,291 Japanese and 586 Korean samples, 1,191 Japanese individuals and all 586 Korean individuals were included in our previous study [9]. With regard to additional Japanese individuals, we collected samples from 48 healthy controls at Kohnodai Hospital, and 52 HBV patients at Okayama University Hospital and Ehime University Hospital, including 26 individuals with LC and 26 individuals with HCC. A total of 661 Hong Kong samples and 629 Thai samples were collected at Queen Mary Hospital and Chulalongkorn University, respectively.

HBV status was measured based on serological results for HBsAg and anti-HBc with a fully automated chemiluminescent enzyme immunoassay system (Abbott ARCHITECT; Abbott Japan, Tokyo, Japan, or LUMIPULSE f or G1200; Fujirebio, Inc., Tokyo, Japan). For clinical staging, inactive carrier (IC) state was defined by the presence of HBsAg with normal ALT levels over 1 year (examined at least four times at 3-month intervals) and without evidence of liver cirrhosis. Chronic hepatitis (CH) was defined by elevated ALT levels (>1.5 times the upper limit of normal [35 IU/L]) persisting over 6 months (by at least 3 bimonthly tests). Acute exacerbation (AE) of chronic hepatitis B was defined as an elevation of ALT to more than 10 times the upper limit of normal (ULN, 58 IU/L) and bilirubin to at least three times ULN (15 μmol/L). LC was diagnosed principally by ultrasonography (coarse liver architecture, nodular liver surface, blunt liver edges and hypersplenism), platelet counts<100,000/cm^3, or a combination thereof. Histological confirmation by fine-needle biopsy of the liver was performed as required. HCC was diagnosed by ultrasonography, computerized tomography, magnetic resonance imaging, angiography, tumor biopsy or a combination thereof.

The Japanese control samples from HBV-resolved subjects (HBsAg-negative and anti-HBc-positive) at Nagoya City University-affiliated healthcare center were used by comprehensive agreement (anonymization in a de-identified manner) in this study. Some of the unrelated and anonymized Japanese healthy controls were purchased from the Japan Health Science Research Resources Bank (Osaka, Japan). One microgram of purified genomic DNA was dissolved in 100 μl of TE buffer (pH 8.0) (Wako, Osaka, Japan), followed by storage at −20°C until use.

Genotyping of *HLA-DPA1* and *HLA-DPB1* alleles

High resolution (4-digit) genotyping of *HLA-DPA1* and *-DPB1* alleles was performed for HBV patients, resolved individuals, and healthy controls in Japan, Korea, Hong Kong, and Thailand. LABType SSO HLA DPA1/DPB1 kit (One Lambda, CA) and a Luminex Multi-Analyte Profiling system (xMAP; Luminex, Austin, TX) were used for genotyping, in according with the manufacturer's protocol. Because of the small quantity of genomic DNA in some Korean samples, we performed whole genome amplification for a total of 486 samples using GenomiPhi v2 DNA Amplification kit (GE Healthcare Life Sciences, UK), in accordance with the manufacturer's instruction.

A total of 2,895 samples were successfully genotyped and characteristics of these samples are summarized in Table S1.

Statistical analysis

Fisher's exact test in two-by-two cross tables was used to examine the associations between *HLA-DP* allele and chronic HBV infection or disease progression in chronic HBV patients,

using statistical software R2.9. To avoid false-positive results due to multiple testing, significance levels were adjusted based on the number of observed alleles at each locus in each population. For *HLA-DPA1* alleles, the number of observed alleles was 3 in Japanese, 4 in Korean, 5 in Hong Kong, and 5 in Thai subjects. Therefore, the significant levels for α were set at $\alpha = 0.05/3$ in Japanese, $\alpha = 0.05/4$ in Korean, $\alpha = 0.05/5$ in Hong Kong, and $\alpha = 0.05/5$ in Thai subjects. In the same way, significant levels for *HLA-DPB1* alleles were $\alpha = 0.05/10$, $0.05/11$, $0.05/12$, and $0.05/16$, respectively. Multivariate logistic regression analysis adjusted for age and sex (used as independent variables) was applied to assess associations between the number of *DPB1*02:01* alleles (i.e., 0, 1, or 2) and disease progression in CHB patients. To examine the effect of *DPB1*02:01* allele on disease progression in all populations, population was further adjusted by using three dummy variables (i.e., (c1, c2, c3) = (0, 0, 0) for Japanese, (1, 0, 0) for Korean, (0, 1, 0) for Hong Kong, and (0, 0, 1) for Thai) in a multivariate logistic regression analysis. We obtained the following regression equation: $\text{logit}(p) = -3.905 + 0.083 * \text{age} + (-0.929) * \text{sex} + (-0.684) * \textit{DPB1*02:01} + 1.814 * c1 + (-0.478) * c2 + 0.782 * c3$. Significance levels in the analysis of disease progression in CHB patients were set as $\alpha = 0.05/10$ in Japanese, $\alpha = 0.05/11$ in Korean, $\alpha = 0.05/15$ in Hong Kong, and $\alpha = 0.05/15$ in Thai subjects. The phase of each individual (i.e., a combination of two *DPA1-DPB1* haplotypes) was estimated using PHASE software [21], assuming samples are selected randomly from a general population. In comparison of the estimated *DPA1-DPB1* haplotype frequencies, significant levels were set as $\alpha = 0.05/14$ in Japanese, $\alpha = 0.05/17$ in Korean, $\alpha = 0.05/17$ in Hong Kong, and $\alpha = 0.05/18$ in Thai subjects. Meta-analysis was performed using the DerSimonian-Laird method (random-effects model) in order to calculate pooled OR and its 95% confidence interval (95% CI). We applied meta-analysis for alleles with frequency>1% in all four Asian populations. The significance levels in meta-analysis were adjusted by the total number of statistical tests; $\alpha = 0.05/20$ for *DPA1* alleles, $\alpha = 0.05/57$ for *DPB1* alleles, and $\alpha = 0.05/74$ for *DPA1-DPB1* haplotypes.

Supporting Information

Figure S1 Comparison of odds ratios in association analyses for *HLA-DP* with chronic HBV infection among four Asian populations: (A) *HLA-DPA1* alleles; (B) *HLA-DPB1* alleles; and (C) *HLA DPA1-DPB1* haplotypes. Meta-analysis was performed using the DerSimonian-Laird method (random-effects model) to calculate pooled OR and its 95% confidence interval (95% CI). Bold depicts a statistically significant association after correction of significance level.
(DOCX)

Table S1 Individuals with successfully genotyped for *HLA-DPA1* and *HLA-DPB1*.
(DOCX)

Table S2 Frequencies of HLA-DP alleles in HBV patients and healthy controls among Asian populations.
(XLSX)

Table S3 Frequencies of HLA-DP alleles in HBV patients and resolved individuals among Asian populations.
(XLSX)

Table S4 Associations of HLA-DPB1 alleles with disease progression in CHB patients among Asian populations.
(XLSX)

Table S5 Estimated frequencies of HLA DPA1-DPB1 haplotypes in HBV patients and healthy controls among Asian populations.
(XLSX)

Acknowledgments

We would like to thank all the patients and families who contributed to the study. We are also grateful to Ms. Mayumi Ishii (National Center for Global Health and Medicine), Ms. Megumi Sageshima, Yuko Hirano, Natsumi Baba, Rieko Shirahashi, Ayumi Nakayama (University of Tokyo), and Yuko Ohara (Japanese Red Cross Kanto-Koshinetsu Block Blood Center) for technical assistance.

Author Contributions

Conceived and designed the experiments: NN HS MS KT M. Mizokami. Performed the experiments: NN HS KK Y. Mawatari M. Kawashima M. Minami. Analyzed the data: NN HS M. Kawashima JO. Contributed reagents/materials/analysis tools: W-KS M-FY NP YP SHA K-HH K. Matsuura YT M. Kurosaki YA NI J-HK SH TI KY IS Y. Murawaki YI AT EO YH MH SK EM KS KH ET SM MW YE NM K. Murata M. Korenaga KT M. Mizokami. Wrote the paper: NN HS JO KT M. Mizokami.

References

1. Chen DS (1993) From hepatitis to hepatoma: lessons from type B viral hepatitis. Science 262: 369–370.
2. Custer B, Sullivan SD, Hazlet TK, Iloeje U, Veenstra DL, et al. (2004) Global epidemiology of hepatitis B virus. J Clin Gastroenterol 38: S158–168.
3. Zidan A, Scheuerlein H, Schule S, Settmacher U, Rauchfuss F (2012) Epidemiological pattern of hepatitis B and hepatitis C as etiological agents for hepatocellular carcinoma in iran and worldwide. Hepat Mon 12: e6894.
4. Pungpapong S, Kim WR, Poterucha JJ (2007) Natural history of hepatitis B virus infection: an update for clinicians. Mayo Clin Proc 82: 967–975.
5. Kim DW, Lee SA, Hwang ES, Kook YH, Kim BJ (2012) Naturally occurring precore/core region mutations of hepatitis B virus genotype C related to hepatocellular carcinoma. PLoS One 7: e47372.
6. Jiang DK, Sun J, Cao G, Liu Y, Lin D, et al. (2013) Genetic variants in STAT4 and HLA-DQ genes confer risk of hepatitis B virus-related hepatocellular carcinoma. Nat Genet 45: 72–75.
7. Kamatani Y, Wattanapokayakit S, Ochi H, Kawaguchi T, Takahashi A, et al. (2009) A genome-wide association study identifies variants in the HLA-DP locus associated with chronic hepatitis B in Asians. Nat Genet 41: 591–595.
8. Mbarek H, Ochi H, Urabe Y, Kumar V, Kubo M, et al. (2011) A genome-wide association study of chronic hepatitis B identified novel risk locus in a Japanese population. Hum Mol Genet 20: 3884–3892.
9. Nishida N, Sawai H, Matsuura K, Sugiyama M, Ahn SH, et al. (2012) Genome-wide association study confirming association of HLA-DP with protection against chronic hepatitis B and viral clearance in Japanese and Korean. PLoS One 7: e39175.
10. Guo X, Zhang Y, Li J, Ma J, Wei Z, et al. (2011) Strong influence of human leukocyte antigen (HLA)-DP gene variants on development of persistent chronic hepatitis B virus carriers in the Han Chinese population. Hepatology 53: 422–428.
11. An P, Winkler C, Guan L, O'Brien SJ, Zeng Z (2011) A common HLA-DPA1 variant is a major determinant of hepatitis B virus clearance in Han Chinese. J Infect Dis 203: 943–947.
12. Li J, Yang D, He Y, Wang M, Wen Z, et al. (2011) Associations of HLA-DP variants with hepatitis B virus infection in southern and northern Han Chinese populations: a multicenter case-control study. PLoS One 6: e24221.
13. Vermehren J, Lotsch J, Susser S, Wicker S, Berger A, et al. (2012) A common HLA-DPA1 variant is associated with hepatitis B virus infection but fails to distinguish active from inactive Caucasian carriers. PLoS One 7: e32605.
14. Sawai H, Nishida N, Mbarek H, Matsuda K, Mawatari Y, et al. (2012) No association for Chinese HBV-related hepatocellular carcinoma susceptibility SNP in other East Asian populations. BMC Med Genet 13: 47.
15. Chandanayingyong D, Stephens HA, Fan L, Sirikong M, Longta P, et al. (1994) HLA-DPB1 polymorphism in the Thais of Southeast Asia. Hum Immunol 40: 20–24.

16. Chandanayingyong D, Stephens HA, Klaythong R, Sirikong M, Udee S, et al. (1997) HLA-A, -B, -DRB1, -DQA1, and -DQB1 polymorphism in Thais. Hum Immunol 53: 174–182.
17. Maneemaroj R, Stephens HA, Chandanayingyong D, Longta K, Bejrachandra S (1997) HLA class II allele frequencies in northern Thais (Kamphaeng Phet). J Med Assoc Thai 80 Suppl 1: S20–24.
18. Wu TW, Chu CC, Ho TY, Chang Liao HW, Lin SK, et al. (2013) Responses to booster hepatitis B vaccination are significantly correlated with genotypes of human leukocyte antigen (HLA)-DPB1 in neonatally vaccinated adolescents. Hum Genet.
19. Hu L, Zhai X, Liu J, Chu M, Pan S, et al. (2012) Genetic variants in human leukocyte antigen/DP-DQ influence both hepatitis B virus clearance and hepatocellular carcinoma development. Hepatology 55: 1426–1431.
20. Li S, Qian J, Yang Y, Zhao W, Dai J, et al. (2012) GWAS identifies novel susceptibility loci on 6p21.32 and 21q21.3 for hepatocellular carcinoma in chronic hepatitis B virus carriers. PLoS Genet 8: e1002791.
21. Stephens M, Smith NJ, Donnelly P (2001) A new statistical method for haplotype reconstruction from population data. Am J Hum Genet 68: 978–989.

The American Journal of Pathology, Vol. 184, No. 11, November 2014

ELSEVIER

The American Journal of
PATHOLOGY
ajp.amjpathol.org

GASTROINTESTINAL, HEPATOBILIARY, AND PANCREATIC PATHOLOGY

Hepatitis C Virus Core Protein Suppresses Mitophagy by Interacting with Parkin in the Context of Mitochondrial Depolarization

Yuichi Hara,* Izumi Yanatori,† Masanori Ikeda,‡ Emi Kiyokage,§ Sohji Nishina,* Yasuyuki Tomiyama,* Kazunori Toida,§ Fumio Kishi,† Nobuyuki Kato,‡ Michio Imamura,¶ Kazuaki Chayama,¶ and Keisuke Hino*

From the Departments of Hepatology and Pancreatology, Molecular Genetics,† and Anatomy,§ Kawasaki Medical School, Kurashiki; the Department of Tumor Virology,‡ Okayama University Graduate School of Medicine, Dentistry and Pharmaceutical Sciences, Okayama; and the Department of Gastroenterology and Metabolism,¶ Applied Life Sciences, Institute of Biomedical and Health Sciences, Hiroshima University, Hiroshima, Japan*

Accepted for publication July 25, 2014.

Address correspondence to Keisuke Hino, M.D., Ph.D., Department of Hepatology and Pancreatology, Kawasaki Medical School, 577 Matsushima, Kurashiki, Okayama 701-0192, Japan. E-mail: khino@med.kawasaki-m.ac.jp.

Hepatitis C virus (HCV) causes mitochondrial injury and oxidative stress, and impaired mitochondria are selectively eliminated through autophagy-dependent degradation (mitophagy). We investigated whether HCV affects mitophagy in terms of mitochondrial quality control. The effect of HCV on mitophagy was examined using HCV-Japanese fulminant hepatitis-1–infected cells and the uncoupling reagent carbonyl cyanide *m*-chlorophenylhydrazone as a mitophagy inducer. In addition, liver cells from transgenic mice expressing the HCV polyprotein and human hepatocyte chimeric mice were examined for mitophagy. Translocation of the E3 ubiquitin ligase Parkin to the mitochondria was impaired without a reduction of pentaerythritol tetranitrate–induced kinase 1 activity in the presence of HCV infection both *in vitro* and *in vivo*. Coimmunoprecipitation assays revealed that Parkin associated with the HCV core protein. Furthermore, a Yeast Two-Hybrid assay identified a specific interaction between the HCV core protein and an N-terminal Parkin fragment. Silencing Parkin suppressed HCV core protein expression, suggesting a functional role for the interaction between the HCV core protein and Parkin in HCV propagation. The suppressed Parkin translocation to the mitochondria inhibited mitochondrial ubiquitination, decreased the number of mitochondria sequestered in isolation membranes, and reduced autophagic degradation activity. Through a direct interaction with Parkin, the HCV core protein suppressed mitophagy by inhibiting Parkin translocation to the mitochondria. This inhibition may amplify and sustain HCV-induced mitochondrial injury. *(Am J Pathol 2014, 184: 3026–3039; http://dx.doi.org/10.1016/j.ajpath.2014.07.024)*

Oxidative stress is present in chronic hepatitis C to a greater degree than in other inflammatory liver diseases.[1,2] The hepatitis C virus (HCV) core protein induces the production of reactive oxygen species (ROS)[3,4] through mitochondrial electron transport inhibition.[5] Because the mitochondria are targets for ROS and ROS generators, HCV-induced ROS have the potential to injure mitochondria. In addition, hepatocellular mitochondrial alterations have been observed in patients with chronic hepatitis C.[6] We previously identified a ROS-associated iron metabolic disorder[7] and demonstrated that transgenic mice expressing the HCV polyprotein develop hepatocarcinogenesis related to mitochondrial injury induced by HCV and iron overload.[8] Therefore, impaired mitochondrial function may play a critical role in the development of hepatocellular carcinoma (HCC) in patients with chronic HCV infection. Conversely, the affected mitochondria are selectively eliminated through the autophagy-dependent degradation of mitochondria (referred to as mitophagy) in both physiological and pathological settings to maintain the mitochondrial quality.[9,10] On the

Supported by Japan Society for the Promotion of Science Grant-in-Aid for Scientific Research (B) 23390201 and Grant-in-Aid for Exploratory Research 25670374; Ministry of Health, Labor and Welfare of Japan Health and Labor Sciences Research grant 25200601 for research on hepatitis; and Kawasaki Medical School Research Project grant P2.

Disclosures: None declared.

Current address of M.I., Kagoshima University Graduate School of Medical and Dental Sciences, Kagoshima, Japan.

http://dx.doi.org/10.1016/j.ajpath.2014.07.024

basis of these observations, we hypothesized that HCV may suppress mitophagy, which could lead to the sustained presence of affected mitochondria, increased ROS production, and the development of HCC.

Mitochondrial membrane depolarization precedes mitophagy induction,[11] which is selectively controlled by a variety of proteins in mammalian cells, including pentaerythritol tetranitrate–induced kinase 1 (PINK1) and the E3 ubiquitin ligase Parkin.[12–19] PINK1 facilitates Parkin targeting of the depolarized mitochondria.[12–15] Although Parkin ubiquitinates a broad range of mitochondrial outer membrane proteins,[14,17–19] it remains unclear how Parkin enables the damaged mitochondria to be recognized by the autophagosome. Structures containing autophagy-related protein 9A and the uncoordinated family member-51–like kinase 1 complex independently target depolarized mitochondria at the initial stages of Parkin-mediated mitophagy, whereas the autophagosomal microtubule-associated protein light chain 3 (LC3) is critical for efficient incorporation of damaged mitochondria into the autophagosome at a later stage.[20] LC3-I undergoes post-translational modification by phosphatidylethanolamine to become LC3-II, and LC3-II insertion into the autophagosomal membrane is a key step in autophagosome formation. In addition, the autophagic adaptor p62 is recruited to mitochondrial clusters and is essential for mitochondrial clearance,[13] although it remains controversial as to whether p62 is essential for mitochondrial recognition by the autophagosome[13] or rather is important for perinuclear clustering of depolarized mitochondria.[19,21] Our aim was to examine whether HCV suppresses mitophagy. We found that HCV core protein inhibits the translocation of Parkin to affected mitochondria by interacting with Parkin and subsequently suppressing mitophagy. These results imply that mitochondria affected by HCV core protein are unlikely to be eliminated, which may intensify oxidative stress and increase the risk of hepatocarcinogenesis.

Materials and Methods

Cell Culture, HCV Infection Experiments, and Mitochondrial Depolarization

HCV-Japanese fulminant hepatitis-1 (JFH1)–infected Huh7 cells have previously been described in detail.[22] The supernatants were collected from cell culture–generated JFH1-Huh7 cells at 21 days after infection and stored until use at −80°C after filtering through a 0.45-μm filter. For infection experiments with the HCV-JFH1 virus, 1×10^5 Huh7 cells per well were plated onto 6-well plates and cultured for 24 hours. Then, we infected the cells with 50 μL (equivalent to a multiplicity of infection of 0.1) of inoculum. The culture supernatants were collected, and the levels of the HCV core were determined using an enzyme-linked immunosorbent assay (ELISA; Mitsubishi Kagaku Bio-Clinical Laboratories, Tokyo, Japan). Total RNA was isolated from the infected cellular lysates using an RNeasy mini kit (Qiagen, Hilden, Germany) for quantitative RT-PCR analysis of the intracellular HCV RNA. The HCV infectivity in the culture supernatants was determined by a focus-forming assay at 48 hours after infection. The HCV-infected cells were detected using an anti-HCV core antibody (CP-9 and CP-11, Institute of Immunology, Ltd, Tokyo, Japan). Intracellular HCV infectivity was determined using a focus-forming assay at 48 hours after inoculation of the lysates by repeated freeze-and-thaw cycles (three times).

To depolarize the mitochondria, the cells were treated with 10 μmol/L carbonyl cyanide *m*-chlorophenylhydrazone (CCCP; Sigma-Aldrich, St. Louis, MO) for 1 to 2 hours or 1 μmol/L valinomycin (Sigma-Aldrich) for 3 hours; CCCP represses ATP synthesis through the loss of the H^+ gradient without affecting mitochondrial electron transport, which is known to induce mitochondrial fragmentation.[13]

Animals

The pAlbSVPA-HCV vector, which contains the full-length polyprotein-coding region under the control of the murine albumin promoter/enhancer, has previously been described in detail.[23,24] Of the four transgenic lineages with evidence of RNA transcription of the full-length HCV-N open reading frame (FL-N), the FL-N/35 lineage proved capable of breeding large numbers.[24] Urokinase-type plasminogen activator–transgenic severe combined immunodeficiency mice were generated, and human hepatocytes were transplanted to generate chimeric mice.[25] The chimeric mice were injected with genotype *1b* HCV-positive human serum samples, as described previously.[26] The mouse livers were extracted 12 weeks after the infection, when the serum HCV RNA titers had increased over baseline levels. Male FL-N/35 transgenic mice, age-matched C57BL/6 mice (control), and chimeric mice with and without HCV infection were fed, maintained, and then euthanized by i.p. injection of 10% nembutal sodium, according to the guidelines approved by the Institutional Animal Care and Use Committee. The study protocol for obtaining human serum samples conformed to the ethical guidelines of the 1975 Declaration of Helsinki and was approved by the Institutional Review Committee.

Measurement of HCV RNA and Human Albumin in the Serum of Chimeric Mice

HCV RNA[26] and human albumin[25] were quantified as described previously. Human albumin levels in the serum of chimeric mice were determined using the Human Albumin ELISA Quantification kit (Bethyl Laboratories Inc., Montgomery, TX).

Measurement of Mitochondrial Membrane Potential

The mitochondrial membrane potential ($\Delta\Psi$) was measured using a Cell Meter JC-10 Mitochondrial Membrane Potential Assay kit (AAT Bioquest, Inc., Sunnyvale, CA), according to the manufacturer's instructions. The fluorescent intensities

for both J-aggregates (red) and monometric forms (green) of JC-10 were measured at Ex/Em = 490/525 nm and 540/590 nm with a Varioskan Flush Multimode Reader (Thermo Fisher Scientific, Waltham, MA).

Isolation of Mitochondria

The cells were lysed by mechanical homogenization using a small pestle, and mitochondrial extraction was performed using a Qproteome Mitochondria Isolation kit (Qiagen), according to the manufacturer's instructions. Liver mitochondria were isolated as described previously with some modifications.[27] In brief, the livers were minced on ice and homogenized by five strokes with a Dounce homogenizer and a tight-fitting pestle in isolation buffer [70 mmol/L sucrose, 1 mmol/L KH_2PO_4, 5 mmol/L HEPES, 220 mmol/L mannitol, 5 mmol/L sodium succinate, and 0.1% bovine serum albumin (BSA), pH 7.4]. The homogenate was centrifuged at 800 × *g* for 5 minutes at 4°C. The supernatant fraction was retained, whereas the pellet was washed with isolation buffer and centrifuged again. The combined supernatant fractions were centrifuged at 1000 × *g* for 15 minutes at 4°C to obtain a crude mitochondrial pellet.

Measurement of ROS

The cellular ROS level was measured by oxidation of the cell-permeable, oxidation-sensitive fluorogenic precursor, *2′,7′*-dihydrodichlorofluorescein diacetate (Molecular Probes Inc., Eugene, OR). Fluorescence was measured using a Varioskan Flush Multimode Reader at 495/535 nm (excitation/emission).

Determination of Glutathione Content

Mitochondrial pellets were measured for total glutathione [reduced glutathione (GSH) + oxidized glutathione (GSSG)] and GSH content using the GSSG/GSH Quantification kit (Dojindo Molecular Technologies, Inc., Kumamoto, Japan). The concentration of GSH was calculated using the following formula:

$$\text{GSH concentration} = \text{Total glutathione concentration} - [\text{GSSG concentration}] \times 2 \quad (1)$$

The liver tissue samples (approximately 50 mg) were minced in ice-cold metaphosphoric acid solution, homogenized, and centrifuged at 3000 × *g* for 10 minutes at 4°C. Lysates from the liver tissue samples and mitochondrial samples (2 mg) were evaluated for the concentration of GSH using the thioester method and a GSH-400 kit (Oxis International Inc., Portland, OR) and for total glutathione content using the glutathione reductase–dinitrothiocyanobenzene recycling assay and the GSH-412 kit (Oxis International Inc.), as described previously.[5]

Immunoblotting

Samples were lysed in radioimmunoprecipitation assay buffer [20 mmol/L Tris-HCl (pH 7.5), 150 mmol/L NaCl, 50 mmol/L NaF, 1 mmol/L Na_3VO_4, 0.1% SDS, and 0.5% Triton X-100], as described previously,[28] supplemented with 1% protease inhibitor mixture (Sigma-Aldrich) and 100 mmol/L phenylmethylsulfonyl fluoride. Cell lysates or mitochondrial pellets were subjected to immunoblot analysis using an iBlot Gel Transfer Device (Invitrogen, Carlsbad, CA). The membranes were incubated with the following primary antibodies: rabbit anti-human LC3 (Novus Biologicals, Littleton, CO), rabbit anti-human p62/SQSTM1 (MBL, Nagoya, Japan), rabbit anti-human Parkin (Cell Signaling Technology, Danvers, MA), mouse anti-human Parkin (Santa Cruz Biotechnology, Inc.), rabbit anti-human p-Parkin (Ser 378; Santa Cruz Biotechnology, Inc.), rabbit anti-human PINK1 (Cell Signaling Technology), mouse anti-human mitochondrial heat shock protein-70 (BioReagents, Golden, CO), mouse anti-human ubiquitin (Santa Cruz Biotechnology, Inc.), goat anti-human voltage-dependent anion-selective channel protein 1 (VDAC1; Santa Cruz Biotechnology, Inc.), monoclonal antisynthetic HCV core peptide (CP11; Institute of Immunology, Ltd), mouse anti-HCV non-structural (NS) 3 protein (Abcam, Cambridge, MA), mouse anti-HCV NS4A (Abcam), mouse anti-HCV NS5A protein (Abcam), and rabbit anti-human β-actin (Cell Signaling Technology).

Electron Microscopy

To address the detail localization of core and Parkin, the cells treated with CCCP for 1 hour were fixed with 4% paraformaldehyde and 1% glutaraldehyde in 0.1 mol/L Millonig's phosphate buffer (pH 7.4) for 30 minutes. The cells were incubated with a mixture of the following primary antibodies in phosphate-buffered saline (PBS) containing 1% BSA and 0.05% sodium azide overnight at 20°C: mouse monoclonal antisynthetic HCV core peptide (Institute of Immunology), rabbit anti-human Parkin (Abcam), and rabbit anti-rat LC3 (Wako Pure Chemical Industries, Ltd, Osaka, Japan). After washing with PBS, the cells were incubated with biotinylated donkey anti-rabbit IgG (Jackson ImmunoResearch Laboratories, Inc., Baltimore Pike, PA) in 1% BSA for 2 hours at 20°C. After washing with PBS, the cells were incubated with Alexa Fluor-488 FluoroNanogold-streptavidin (Jackson ImmunoResearch Laboratories, Inc.), indocarbocyanine-labeled donkey anti-mouse IgG (Jackson ImmunoResearch Laboratories, Inc.), and indocarbocyanine-labeled donkey anti-rabbit IgG (Jackson ImmunoResearch Laboratories, Inc.) in 1% BSA for 2 hours at 20°C. After washing with PBS, the cells were incubated with mouse peroxidase–anti-peroxidase complex (Jackson ImmunoResearch Laboratories, Inc.) in PBS for 3 hours at 20°C. The peroxidase reduction was developed with 0.05% diaminobenzidine tetrahydrochloride in 50 mmol/L Tris buffer containing 0.01% hydrogen peroxide for 20 minutes at room temperature. The diameter of the gold immunoparticles was increased using a silver enhancement kit (HQ silver; Nanoprobes, Inc., Yaphank, NY) for 4 minutes at

room temperature. After treatment with 1% osmium and 2% uranyl acetate, the cells were dehydrated in a graded series of ethanol and embedded in Epon-Araldite (OKEN, Tokyo, Japan). Serial ultrathin sections (each 70 nm thick) were examined using an electron microscope (model JEM1400; JEOL, Tokyo, Japan). These immune–electron microscopic methods were generally performed according to our previous study.[29]

Immunofluorescence Microscopy

The cells were fixed, permeabilized, and immunostained with rabbit anti-human Parkin (Abcam), goat anti-human Parkin (Santa Cruz Biotechnology, Inc.), goat anti-human Tom20 (Santa Cruz Biotechnology, Inc.), rabbit anti-rat LC3 (Wako Pure Chemical Industries, Ltd), or mouse monoclonal anti-synthetic HCV core peptide (Institute of Immunology) antibodies, followed by Cy3-conjugated donkey anti-rabbit IgG (Jackson ImmunoResearch Laboratories, Inc.), fluorescein isothiocyanate–conjugated donkey anti-goat IgG (Jackson ImmunoResearch Laboratories, Inc.), or Alexa Fluor 647–conjugated donkey anti-mouse IgG (Jackson ImmunoResearch Laboratories, Inc.). Cell images were captured using a confocal microscope (model LSM700; Zeiss, Jena, Germany) equipped with 488-, 555-, and 639-nm diodes. The images were acquired in a sequential mode using a 63× Plan Apochromat numerical aperture/1.4 oil objective and the appropriate filter combinations. All images were saved as tagged image file format files. The contrast was adjusted using Photoshop version CS5 (Adobe, San Jose, CA), and the images were imported into Illustrator version CS5 (Adobe). Colocalization was assessed with line scans using ImageJ software version 1.46 (NIH, Bethesda, MD).

Coimmunoprecipitation

Coimmunoprecipitation was performed using a Dynabeads Co-Immunoprecipitation Kit (Invitrogen), according to the manufacturer's instructions. Magnetic beads (Dynabeads M-270 Epoxy) were conjugated to anti-VDAC1 (Santa Cruz Biotechnology, Inc.), anti-Parkin (Cell Signaling Technology), anti-ubiquitin (Santa Cruz Biotechnology, Inc.), or anti-p62 (MBL) antibodies by rotating overnight at 37°C. The antibody-Dynabeads complex was then treated with coupling buffer. Beads coupled to anti-VDAC, anti-Parkin, anti-ubiquitin, or anti-p62 were incubated with cell lysates for 30 minutes at 4°C and then washed with coupling buffer. Collected protein complexes were subjected to immunoblot analysis using anti-VDAC, anti-ubiquitin (Santa Cruz Biotechnology, Inc.), and anti-Parkin (Cell Signaling Technology) antibodies to detect coimmunoprecipitated VDAC1, ubiquitin, and Parkin. Immunoblots using anti-Parkin, anti-HCV core (Institute of Immunology), anti-HCV NS3 (Abcam), anti-HCV NS4A (Abcam), or anti-HCV NS5A (Abcam) antibodies were performed to detect the coimmunoprecipitation of Parkin with core, NS3, NS4A, or NS5A protein.

RNA Interference

The siRNA knockdown oligonucleotides were obtained from Invitrogen. JFH1-Huh7 cells and/or Huh7 cells were grown to 50% to 60% confluency and transfected with 100 pmol siRNA oligonucleotides [5′-GGACGCUGUUCCUCGUUAUGAA-GAA-3′ (forward) and 5′-UUCUUCAUAACGAGGAACA-GCGUCC-3′ (reverse)] for PINK1 or siRNA oligonucleotides [5′-UCCAGCUCAAGGAGGUGGUUGCUAA-3′ (forward) and 5′-UUAGCAACCACCUCCUUGAGCUGGA-3′ (reverse)] for Parkin using Lipofectamine 2000 (Invitrogen). The cells were analyzed 72 hours after transfection.

Yeast Two-Hybrid Assay

A Matchmaker Gal4 two-hybrid system 3 (Clontech Laboratories, Inc., Mountain View, CA) was used according to the manufacturer's instructions. *Saccharomyces cerevisiae* Y187, containing an N- or C-terminal fragment cDNA of Parkin as a prey cloned into the Gal4-activation domain vector (pACT2), was allowed to mate with *S. cerevisiae* AH109, which had been transformed with a Gal4 DNA-binding domain vector (pGBKT7) containing the HCV core as bait. In addition, *S. cerevisiae* Y187, with the HCV core as a prey cloned into the Gal4-activation domain vector (pACT2), was allowed to mate with *S. cerevisiae* AH109, which had been transformed with a Gal4 DNA-binding domain vector (pGBKT7) containing N- or C-terminal fragment cDNA of Parkin as bait. To construct the prey and the bait, two regions of the Parkin gene that encoded the N-terminal 215–amino acid residues (1 to 215) and the C-terminal 250–amino acid residues (216 to 465) were amplified using PCR with genomic cDNA, and the HCV core gene was amplified with the HCV-O (genotype *1b*) genomic cDNA.[30] The PCR primers were as follows with the incorporated BamHI and EcoRI sites underlined: Parkin 1 to 215, 5′-GGATCCGCATGATAGTGTTTGTCAGGTT-3′ (forward) and 5′-GAATTCCTAGTGTGCTCCACATTTAA-AGA-3′ (reverse); Parkin 216 to 465, 5′-GGATCCGCCC-CACCTCTGACAAGGAAAC-3′ (forward) and 5′-GAAT-TCCTACACGTCGAACCAGTGGT-3′ (reverse); and HCV core, 5′-GAATTCGCCATGAGCACAAATCCTAAACCT-C-3′ (forward) and 5′-GGATCCTTAAGCGGAAGCTGG-GATGGTCAAA-3′ (reverse).

Real-Time RT-PCR

Total RNA was extracted from frozen liver tissues and cells using the RNeasy mini kit (Qiagen). Total RNA (2 μg) was reverse transcribed to cDNA using the High-Capacity RNA to cDNA kit (Applied Biosystems, Foster City, CA), according to the manufacturer's instructions. TaqMan Gene Expression Assays for LC3B, glyceraldehyde-3-phosphate dehydrogenase (GAPDH), Parkin, and HCV core were purchased from Applied Biosystems, and mRNA levels were quantified in triplicate using an Applied Biosystems

7500 Real-Time PCR system, according to the supplier's recommendations. The expression value for LC3B, Parkin, and HCV core mRNA was normalized to that of GAPDH.

Statistical Analysis

Quantitative values are expressed as the means ± SD. Data were compared between the two groups using the Student's *t*-test. $P < 0.05$ was considered significant.

Results

Mitochondrial Oxidative Status *in Vitro* and *in Vivo*

After treatment with CCCP, a widely adopted reagent for inducing mitophagy, the mitochondrial membrane potential ($\Delta\Psi$) was significantly reduced irrespective of HCV infection (Figure 1A). The ratio of reduced/total glutathione content was decreased in the mitochondrial fraction after CCCP treatment in JFH1-Huh7 cells (Figure 1B). Thus, the mitochondrial oxidative status after CCCP treatment was present in HCV-infected cells (JFH1-Huh7). The ratio of reduced/total glutathione content was also decreased in the mitochondrial fraction but not in the whole liver in transgenic mice and HCV-infected chimeric mice compared with the control mice (Figure 1, C and D). These results suggest that there is a baseline oxidation level within the mitochondrial glutathione pool in these transgenic mice and HCV-infected chimeric mice. Furthermore, the mitochondria in these transgenic mice and HCV-infected chimeric mice can undergo mitophagy.

Impaired Recruitment of Parkin to the Mitochondria

Parkin phosphorylation and translocation to the mitochondria after CCCP treatment are indispensable for mitochondrial ubiquitination and subsequent autophagosome formation during the course of mitophagy.[13,15] CCCP exposure induced Parkin accumulation in the mitochondria of Huh7 cells; however, this Parkin recruitment seemed to be inhibited in JFH1-Huh7 cells (Figure 2A). CCCP treatment induces mitochondrial fission, followed by mitophagy.[13] CCCP-treated Huh7 cells displayed fragmented mitochondria colocalized with Parkin, except for a few mitochondrial tubular network cells. Western blot analysis also showed that CCCP-induced recruitment of Parkin to the mitochondria was suppressed without any change in Parkin expression or phosphorylation levels in whole cell lysates of JFH1-Huh7 cells (Figure 2B). Neither CCCP treatment nor HCV infection significantly increased the mRNA levels of Parkin in Huh7 cells, even though there was a tendency of increase in Parkin mRNA after HCV infection (Figure 2C). These results indicate that HCV infection could inhibit Parkin recruitment to CCCP-induced depolarized mitochondria.

The unique and high concentration of CCCP (10 μmol/L) used in the present study may have affected cellular functions

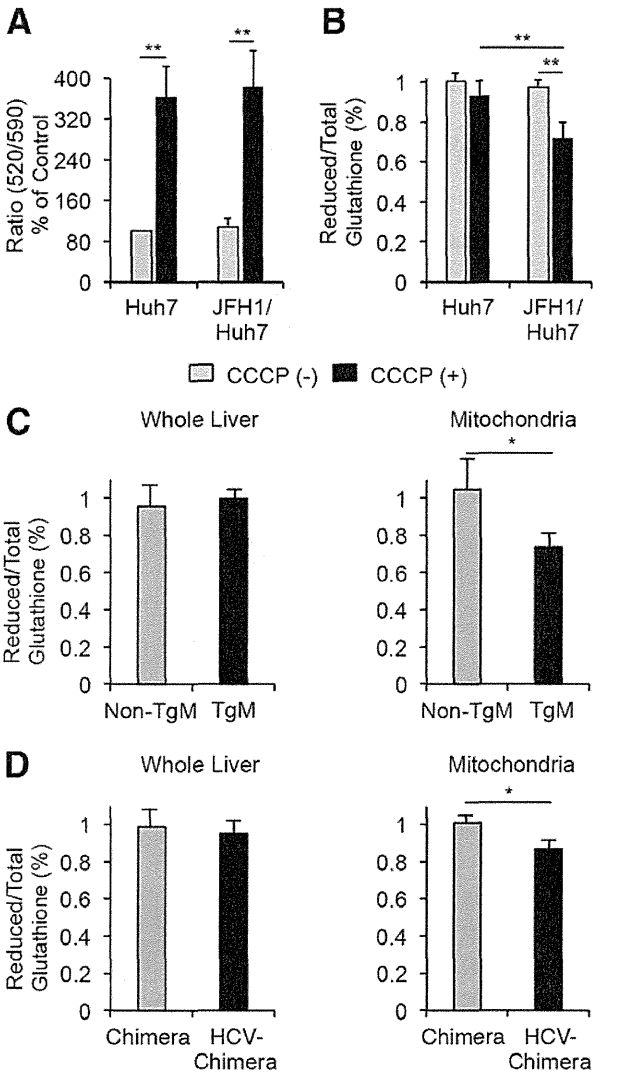

Figure 1 Mitochondrial membrane potential ($\Delta\Psi$) and glutathione content. **A:** Changes in $\Delta\Psi$ levels after a 1-hour carbonyl cyanide *m*-chlorophenylhydrazone (CCCP) treatment for Huh7 and JFH1-Huh7 cells ($n = 5$). The *y* axis represents the ratio of red (JC-10 aggregate form)/green (JC-10 monometric form) fluorescence intensity. **B:** Reduced and total glutathione content in mitochondrial fractions ($n = 5$). Reduced glutathione content was normalized to total glutathione content. Reduced and total glutathione content of freshly isolated whole liver homogenates or mitochondrial fractions of transgenic livers ($n = 7$, **C**) or HCV-infected chimeric mice livers ($n = 5$, **D**) compared with the content in the corresponding control liver samples. Reduced glutathione content was normalized to total glutathione content. $^{*}P < 0.05$, $^{**}P < 0.01$.

other than the proton gradient,[31] which suggests that Parkin translocation from the cytoplasm to the mitochondria may not be induced specifically through mitochondrial depolarization. Therefore, we examined mitochondrial accumulation of Parkin using lower CCCP concentrations (0.1, 1, 5, or 10 μmol/L). In coimmunoprecipitation experiments, CCCP exposure induced ubiquitinated Parkin accumulation in the mitochondria in a dose-dependent manner in Huh7 cells, as described previously,[13] but did not induce these changes in JFH1-Huh7 cells (Figure 2D). These results suggest that

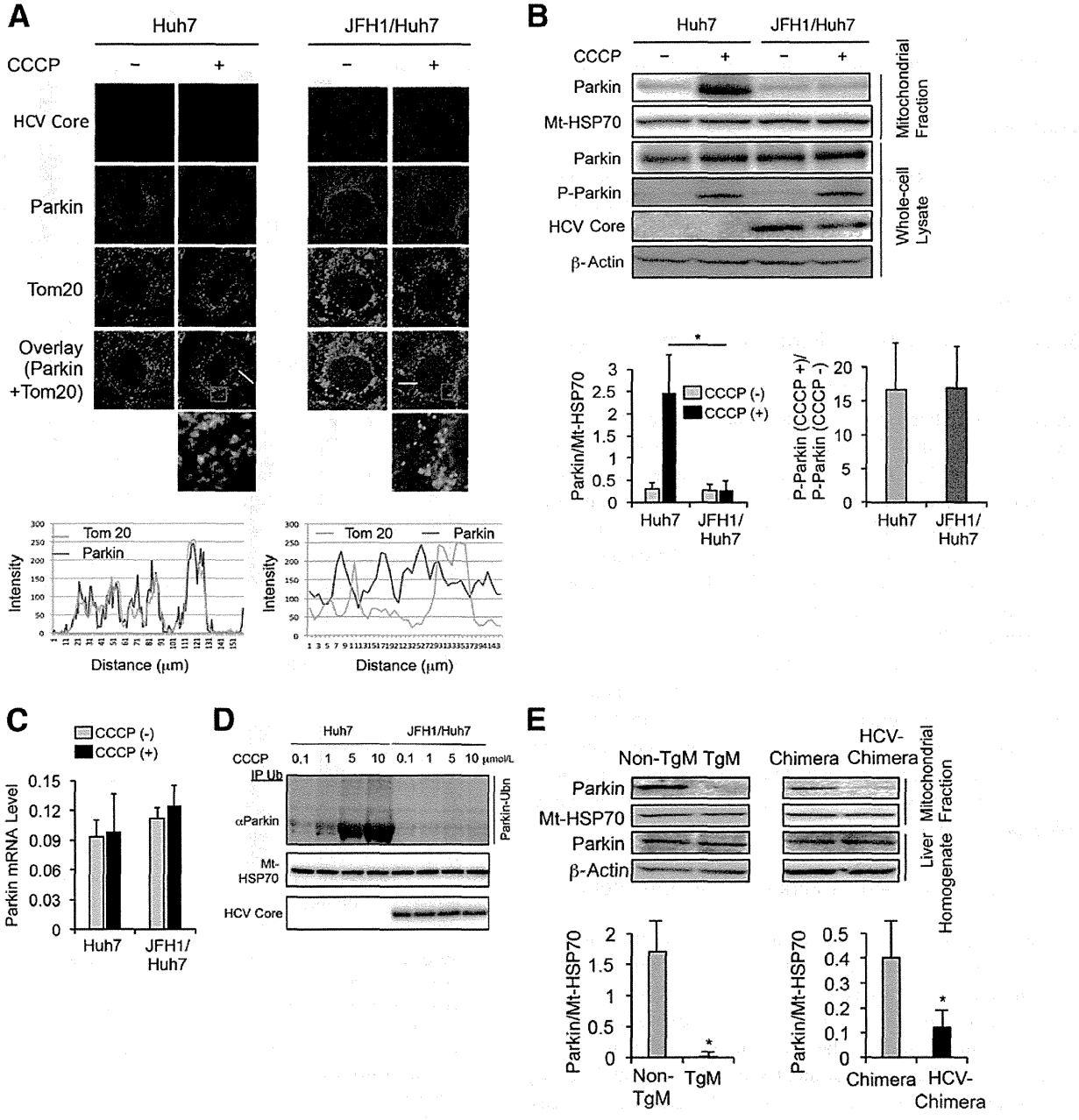

Figure 2 Effect of HCV on the translocation of Parkin to the mitochondria. **A:** Immunofluorescence staining for Parkin (red) and the mitochondrial marker Tom20 (green) in Huh7 and JFH1-Huh7 cells before (−) and after (+) carbonyl cyanide *m*-chlorophenylhydrazone (CCCP) treatment for 1 hour. **Boxed areas** are enlarged below. Endogenous Parkin that colocalizes with the mitochondria (yellow spots). Line scans indicate the colocalization of Parkin with the mitochondria and correlate to the **white lines** in the images. **Boxed areas** are enlarged below. **B:** Immunoblots for Parkin and phosphorylated Parkin (p-Parkin) using the mitochondrial fractions and whole cell lysates before and after CCCP treatment ($n = 5$). Parkin expression level was normalized to mitochondrial heat shock protein 70 (Mt-HSP70). The degree of phosphorylation was expressed as the ratio of phosphorylated Parkin after CCCP treatment to that prior treatment. **C:** Parkin mRNA level in Huh7 cells and JFH1-Huh7 cells before and after CCCP treatment ($n = 5$). The expression level for Parkin was normalized to GAPDH. **D:** Coimmunoprecipitation reveals more ubiquitinated Parkin in CCCP dose-dependent manner in Huh7 cells but not in JFH1-Huh7 cells. **E:** Immunoblots for Parkin using mitochondrial fractions of the livers or liver homogenates from non-TgM and TgM and from chimeric mice with or without HCV infection ($n = 5$ for each type of mouse). $^*P < 0.05$.

CCCP specifically induces mitophagy in Huh7 cells and that the HCV infection has an inhibitory effect on mitophagy in JFH1-Huh7 cells.

FL-N/35-transgenic mice and HCV-infected chimeric mice also showed reduced Parkin expression in the mitochondrial fraction of the liver with no change in Parkin expression levels in whole liver homogenates (Figure 2E). Serum human albumin levels, which serve as useful markers for the extent of replacement with human hepatocytes, were 16.0 ± 7.2 mg/mL in chimeric mice with HCV infection and 11.9 ± 1.7 mg/mL in chimeric mice without HCV infection (Figure 3A). These findings suggest that there was

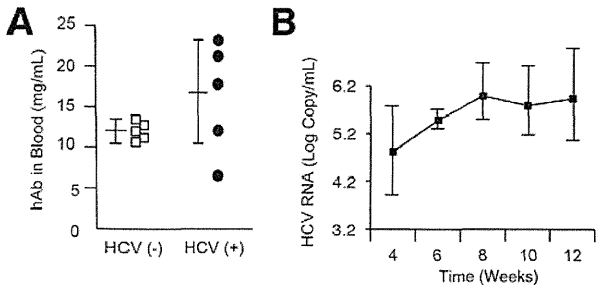

Figure 3 Human albumin and HCV RNA levels in the serum of chimeric mice with or without HCV infection. **A:** Human albumin (hAb) levels in the serum of 3-month-old chimeric mice with or without HCV infection. **B:** Serial change in HCV RNA levels in the serum after HCV infection in chimeric mice ($n = 5$).

a replacement index of >90% according to a graph of the correlation between these two parameters identified in a previous study.[25] Moreover, serum HCV RNA levels increased after infection with HCV (Figure 3B). HCV infection also suppressed the translocation of Parkin to the mitochondria in human hepatocytes.

Interaction between Parkin and the HCV Core Protein

A loss of $\Delta\Psi$ stabilizes the mitochondrial accumulation of PINK1, and PINK1 recruits Parkin from the cytoplasm to depolarized mitochondria via its kinase activity.[11–15] We confirmed that Parkin was phosphorylated to the same degree after CCCP treatment regardless of HCV infection. Therefore, we next examined the mitochondrial accumulation of PINK1. Our results indicate that PINK1 accumulated in the mitochondrial fraction after CCCP treatment, and PINK1 expression levels in whole cell lysates were comparable irrespective of HCV infection (Figure 4A). In addition, blocking PINK1 protein expression with siRNA (Figure 4B) strikingly suppressed Parkin phosphorylation (Figure 4C) and the mitochondrial Parkin signal after CCCP treatment in Huh7 cells (Figure 4D), indicating that PINK1 recruits Parkin from the cytoplasm to depolarized mitochondria via its kinase activity. Suppressed translocation of Parkin to the mitochondria by HCV infection was also confirmed after treatment with valinomycin, a K^+ ionophore that rapidly dissipates $\Delta\Psi$[32] (Figure 4E).

We next examined the association between HCV protein and Parkin and hypothesized that HCV proteins may suppress Parkin translocation to the mitochondria. Coimmunoprecipitation experiments revealed that Parkin associated with the HCV core protein but not other HCV proteins, such as NS3, NS4A, and NS5A, regardless of CCCP treatment (Figure 5A). These results suggest that the HCV core protein specifically suppressed Parkin translocation to impaired mitochondria by interacting with Parkin.

Finally, we investigated which specific Parkin domain is critical for the interaction with the HCV core protein. The proposed Parkin architecture consists of an N-terminal ubiquitin-like domain, a really interesting new gene (RING) 0 domain (RING0), and a C-terminal in-between RING domain[33] (Figure 5B). Of these domains, the RING0 domain and a complete carboxy-terminal RING configuration are critical for the translocation of Parkin to damaged mitochondria and for consequent mitophagy.[13] By using the HCV core protein as bait and either an N-terminal fragment of Parkin, including RING0 (designated Parkin 1 to 215), or a C-terminal fragment of Parkin, not including RING0 (designated Parkin 216 to 465) as prey, a Yeast Two-Hybrid assay identified a specific interaction between Parkin 1 to 215 and the HCV core protein, which was visualized as a strong blue color (activation of the *MEL1* gene encoding

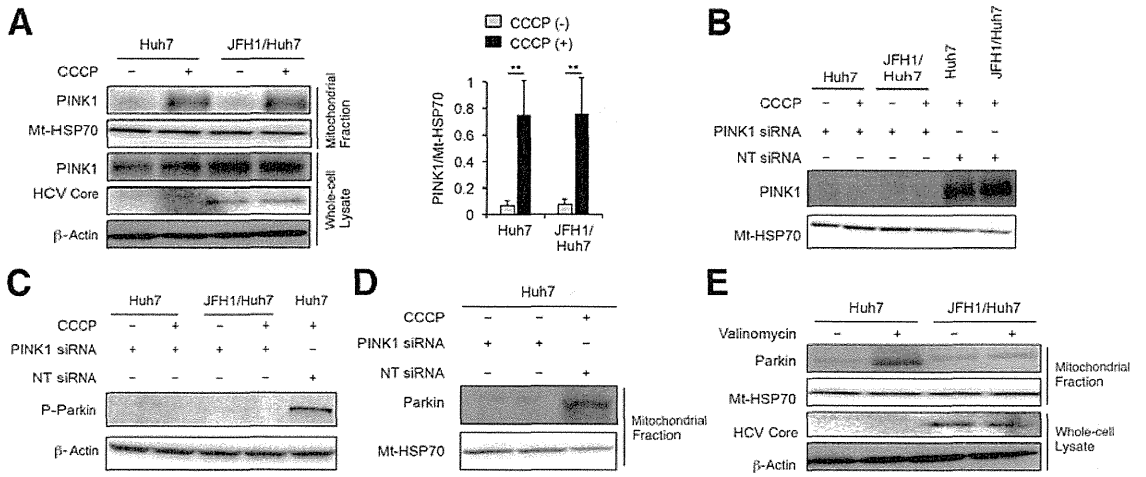

Figure 4 Mitochondrial accumulation of PINK1 after carbonyl cyanide *m*-chlorophenylhydrazone (CCCP) treatment and effect of PINK1 silencing on phosphorylation and mitochondrial translocation of Parkin. **A:** Immunoblots for PINK1 using mitochondrial fractions or whole cell lysates of Huh7 and JFH1-Huh7 cells before and after CCCP treatment ($n = 5$). Immunoblots for PINK1 using mitochondrial fractions (**B**), for phosphorylated Parkin (P-Parkin) using whole cell lysates (**C**), and for Parkin using mitochondrial fractions (**D**) of Huh7 and/or JFH1-Huh7 cells before and after CCCP treatment with or without an siRNA-mediated blockade of PINK1 expression. **E:** Immunoblots for Parkin using the mitochondrial fractions of Huh7 and JFH1-Huh7 cells before and after a 3-hour valinomycin treatment. $^{**}P < 0.01$. Mt-HSP70, mitochondrial heat shock protein 70; NT siRNA, nontargeting siRNA.

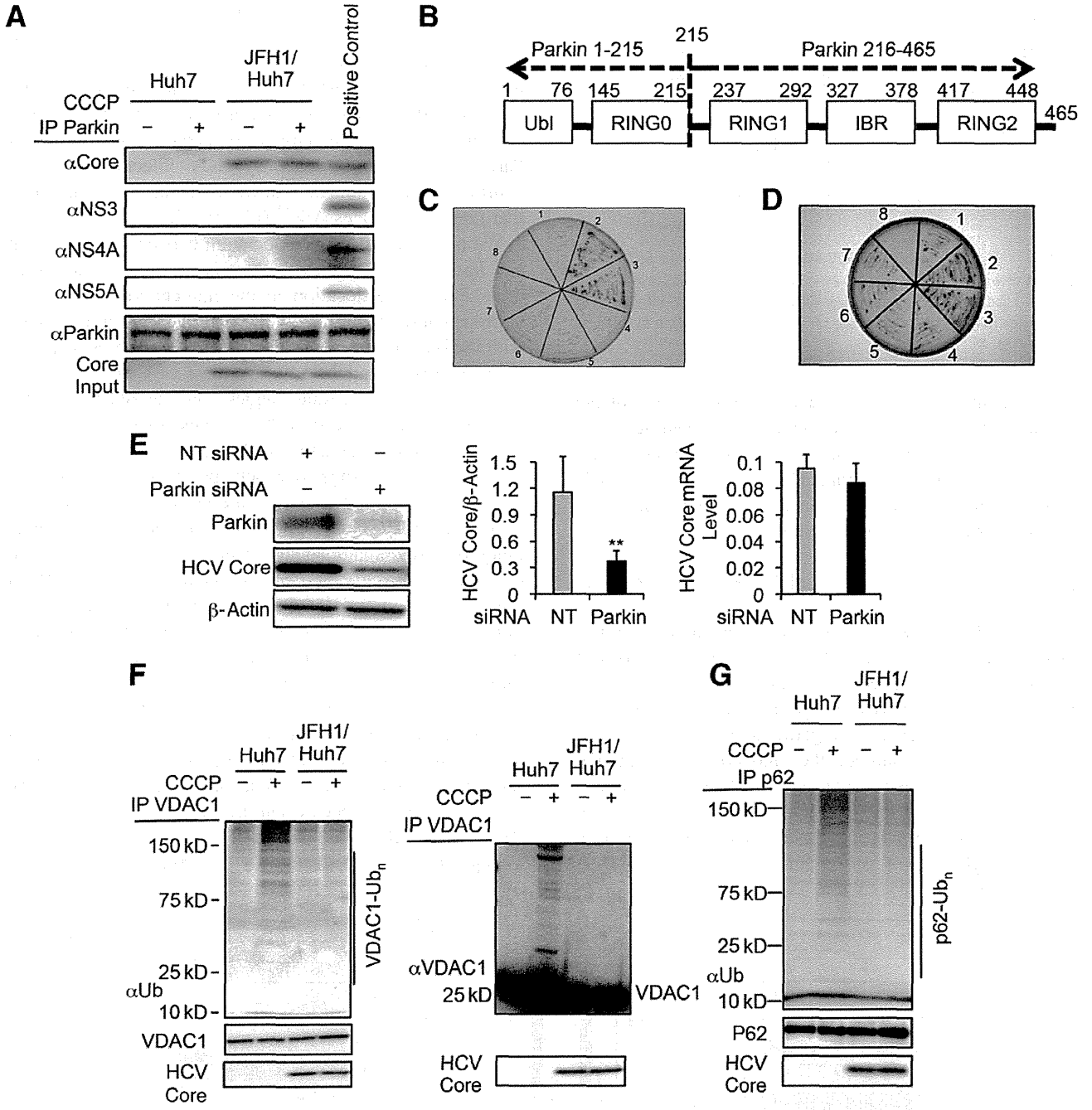

Figure 5 Interaction between Parkin and HCV core protein, effect of Parkin silencing on HCV replication, and reduction of mitochondrial outer membrane ubiquitination. **A:** Coimmunoprecipitation reveals a specific interaction of Parkin with the HCV core protein. **B:** The proposed Parkin architecture and a schematic diagram of Parkin domains. **C** and **D:** A Yeast Two-Hybrid assay identifies a specific interaction between Parkin 1 to 215 and the HCV core protein. The bait and prey for each section (1 to 8) in **C** are as follows: 1, none and none; 2, p53 and large T antigen (positive control); 3, HCV core and Parkin 1 to 215; 4, HCV core and Parkin 216 to 465; 5, HCV core and none; 6, none and Parkin 1 to 215; 7, none and Parkin 216 to 465; 8, no yeast. The bait and prey for each section in **C** were reversed in **D**. **E:** The HCV core protein and HCV core mRNA levels in JFH1-Huh7 cells with or without an siRNA-mediated blockade of Parkin expression ($n = 5$). **F:** Coimmunoprecipitation reveals more VDAC1 ubiquitination in Huh7 cells after carbonyl cyanide m-chlorophenylhydrazone (CCCP) treatment. Various sizes of VDAC1 immunoprecipitates are also detected by immunoblotting using an anti-VDAC1 antibody in Huh7 cells after CCCP treatment. **G:** Coimmunoprecipitation reveals more p62 ubiquitination in Huh7 cells after CCCP treatment. $^{**}P < 0.01$. IBR, in-between RING; NT, nontargeting siRNA; Parkin, Parkin-targeting siRNA; Ubl, ubiquitin-like.

α-galactosidase) (Figure 5C). In contrast, Parkin 216 to 465 did not interact with the HCV core protein. The same results were found when the core protein was used as prey and different domains of Parkin were used as bait (Figure 5D), indicating that this interaction between the two proteins was nonpolar. A previous mutational analysis of Parkin revealed that soluble Parkin mutants K211N, T240R, and G430D do not translocate to the mitochondria.[13] Although we have not

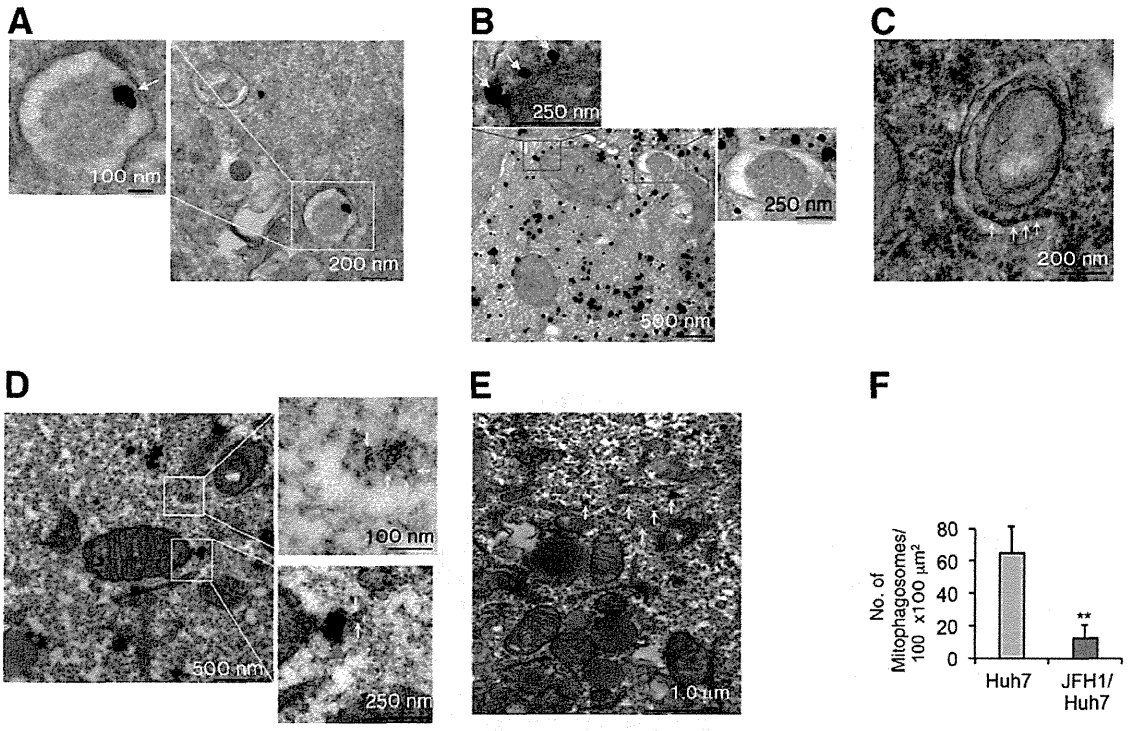

Figure 6 Electron microscopy of Huh7 cells and JFH1-Huh7 cells after carbonyl cyanide *m*-chlorophenylhydrazone (CCCP) treatment. **A–E:** Electron micrographs. **Boxed areas** are enlarged on left (Huh7 cell; **A**), above and on the right (Huh7 cell; **B**), and on the right (JFH1-Huh7 cell; **D**). The **arrows** indicate Parkin labeled with gold on the mitochondrial outer membrane (**A** and **B**), LC3 protein labeled with diaminobenzidine (DAB) on elongating isolation membrane that sequesters a single mitochondrion (Huh7 cells; **C**), Parkin core (**D**), and Parkin labeled with gold (JFH1-Huh7 cell; **E**). The **arrowheads** indicate Parkin labeled with gold (**B**) and HCV core (**D**). **F:** The number of mitophagosomes per 100 × 100 μm^2 was calculated for four randomly selected views. $^{**}P < 0.01$.

determined whether the HCV core protein binds to the region that includes lysine (K) 211 in the RING0 domain, the specific interaction of Parkin 1 to 215 with the HCV core protein raises the possibility that the core protein inhibits Parkin translocation to the mitochondria by affecting lysine 211.

After we confirmed the specific interaction between the HCV core protein and Parkin, we investigated whether Parkin affects HCV replication to investigate the functional role of the interaction between both proteins in the HCV infectious process. Parkin silencing significantly inhibited HCV replication, as indicated by a decrease in HCV core protein expression, but did not affect HCV core mRNA levels (Figure 5E). These results suggest that the association of the HCV core protein with Parkin plays a functional role in HCV propagation, although further studies are required to clarify the mechanisms.

Suppressed Ubiquitination of the Mitochondrial Outer Membrane Protein VDAC1

The next step in mitophagy after Parkin translocation to the mitochondria is the ubiquitination of mitochondrial outer membrane proteins.[13,16] Coimmunoprecipitation experiments revealed that various sizes of ubiquitinated VDAC1 species in the mitochondrial outer membrane[13] were present after CCCP treatment in Huh7 cells but not in JFH1-Huh7 cells (Figure 5F). Western blot analysis of VDAC1 immunoprecipitates revealed various sizes of VDAC1 species after CCCP treatment in Huh7 cells but not in JFH1-Huh7 cells (Figure 5F). The autophagic adaptor p62 aggregates ubiquitinated proteins by polymerizing with other p62 molecules.[13] Similarly, coimmunoprecipitation experiments revealed that CCCP treatment induced various sizes of ubiquitinated p62 species in Huh7 cells but not in JFH1-Huh7 cells (Figure 5G). These results suggest that HCV infection inhibited the Parkin-induced ubiquitination of the depolarized mitochondria.

Suppressed Mitophagosome Formation

During mitophagy, the isolation membrane sequesters a single mitochondrion or a cluster of mitochondria to form an autophagosome (mitophagosome). A single mitochondrion with Parkin on its outer membrane was sequestered by the isolation membrane after CCCP treatment in Huh7 cells (Figure 6A). Parkin in close proximity to the mitochondria and association of Parkin with mitochondrial outer membrane were observed more frequently in Huh7 cells than in JFH1-Huh7 cells (Figure 6, B, D, and E). In addition, LC3 was present on elongating isolation membrane that sequesters a single mitochondrion after CCCP treatment in Huh7 cells (Figure 6C). The number of mitophagosomes, calculated as the number of autophagosomes that contain